OPTIMIZATION OF NATURAL GAS LIQUID (NGL) RECOVERY PROCESSES

by

Balsam Tawfiq Swaidan

A Thesis Presented to the Faculty of the
American University of Sharjah
College of Engineering
in Partial Fulfillment
of the Requirements
for the Degree of

Master of Science in
Chemical Engineering

Sharjah, United Arab Emirates

April 2016

Approval Signatures

We, the undersigned, approve the Master's Thesis of Balsam Tawfiq Swaidan.

Thesis Title: Optimization of Natural Gas Liquid (NGL) Recovery processes

Signature **Date of** (dd/mm/yyyy)

_____ _____
Dr. Rachid Chebbi
Professor, Department of Chemical Engineering
Thesis Advisor

_____ _____
Dr. Zarook Mohamed Shareefdeen
Associate Professor, Department of Chemical Engineering
Thesis Committee Member

_____ _____
Dr. Mohamed Gadalla
Professor, Department of Mechanical Engineering
Thesis Committee Member

_____ _____
Dr. Naif Abdelaziz Darwish
Head
Department of Chemical Engineering

_____ _____
Dr. Mohamed El-Tarhuni
Associate Dean
College of Engineering

_____ _____
Dr. Leland Blank
Dean
College of Engineering

_____ _____
Dr. Khaled Assaleh
Interim Vice Provost for Research and Graduate Studies

Acknowledgements

In the name of Allah, most Gracious, most Merciful. All praise is due to Allah and may His peace and blessings be upon the Prophet (PBUH) for supporting me and guiding me through all the walks of my life and my journey in writing the thesis.

I would like to express my deepest sense of appreciation to my advisor Dr. Rachid Chebbi for his advice, directions and support throughout the course of this thesis. I would also like to acknowledge the committee members and thank them for their useful input.

I would also like to thank the Department of Chemical Engineering at the American University of Sharjah for the educational resources they offer to the graduate students, and for giving me the chance to work as a graduate assistant. Working as a graduate teaching assistant for two years helped me a lot and certainly made me a better chemical engineer.

Last, but not least, I would like to express my sincere gratitude to my parents and family for their unconditional love, support and encouragement throughout this research and in every successful step I made in my life.

Abstract

Natural gas liquid (NGL) is mainly composed of ethane. The demand for ethane is increasing continuously as it is used in the manufacturing of ethylene. A review of the major turboexpansion processes is provided in addition to some related work on the optimization of ethane recovery and profit obtained with several turboexpansion processes. The Cold Residue Recycle (CRR) process was simulated on Aspen HYSYS using lean and rich feed streams at three different demethanizer pressures, namely: 100 psia, 215 psia and 450 psia. The present work aimed at investigating the effect of the split ratios and other design variables on the profit. The optimization of the profit revealed that the Gas Subcooled Process (GSP) is superior to the CRR process in all cases except for lean gas at 100 psia and high NGL to gas price ratio. The external refrigeration requirement was also studied. The findings suggest that external refrigeration is required in all cases except for a lean feed gas operated at 100 psia where self-refrigeration is sufficient in providing the low temperature requirements of the turboexpander process. The flow rate of the splitted streams were included in the optimization. The results also suggest eliminating one splitter in case lean feed is used in the process. Further, the ethane recovery was calculated in all cases confirming that the optimum ethane recoveries available in literature matched the ethane recoveries at optimum profit as well in all cases except for the lean feed at 100 psia where the recovery is slightly below the one available in literature. Furthermore, the effect of CO_2 was studied for all of the GSP cases. The CO_2 tolerance of CRR and GSP was considered at a demethanizer pressure of 100 psia. The findings suggest that CRR is more CO_2 tolerant than GSP.

Search Terms: Natural gas liquids, Cold Residue Recycle process, Gas Subcooled Process, external refrigeration, flowsheet optimization, and optimum profit

Table of Contents

List of Figures

List of Tables

Nomenclature

Natural Gas Liquids	NGLs
Cold Residue Recycle	CRR
Gas Subcooled Process	GSP
Gross Heating Value	GHV
Conventional Turboexpander Process	ISS
Side Draw Reflux Process	SDR
Recycle Vapor Split Process	RVS
Recycle Split Vapor with Enhancement Process	RVSE
Liquid Subcooled Process	LSP
Gas Liquid Subcooled Process	GLSP
Gallons per thousand cubic feet	GPM
Residue Gas Sales	SG
Sales of Natural Gas Liquids	SNGL
Cost of raw material	CRM
Operating cost without depreciation	COM_d
Cost of utilities	C_{UT}
Cost of water treatment	C_{WT}
Cost of operating labor	C_{OL}

Chapter 1. Introduction

1.1. Background

1.1.1. Significance of the research.

Natural gas liquids (NGLs) are composed of ethane, propane, butane, propane, isobutane, pentane and isopentane that are condensed and recovered [1]. The uses for those components are illustrated in Table1. NGL recovery attracts many processing companies due to three reasons. The first reason is to produce a transportable gas stream. This is done to avoid condensation problems during the flow of the two-phase fluid. The second reason is to meet the sales gas specifications. In fact, the main specification for the sales gas is to meet the minimum gross heating value (GHV) while satisfying the hydrocarbon dew point requirement. The third reason is to maximize NGL recovery which is associated with the market trends [2].

NGL Attribute Summary				eia
Natural Gas Liquid	**Chemical Formula**	**Applications**	**End Use Products**	**Primary Sectors**
Ethane	C_2H_6 	Ethylene for plastics production; petrochemical feedstock	Plastic bags; plastics; anti-freeze; detergent	Industrial
Propane	C_3H_8 	Residential and commercial heating; cooking fuel; petrochemical feedstock	Home heating; small stoves and barbeques; LPG	Industrial, Residential, Commercial
Butane	C_4H_{10} 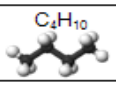	Petrochemical feedstock; blending with propane or gasoline	Synthetic rubber for tires; LPG; lighter fuel	Industrial, Transportation
Isobutane	C_4H_{10} 	Refinery feedstock; petrochemical feedstock	Alkylate for gasoline; aerosols; refrigerant	Industrial
Pentane	C_5H_{12} 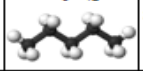	Natural gasoline; blowing agent for polystyrene foam	Gasoline; polystyrene; solvent	Transportation
Pentanes Plus*	Mix of C_5H_{12} and heavier	Blending with vehicle fuel; exported for bitumen production in oil sands	Gasoline; ethanol blends; oil sands production	Transportation

Table 1: Uses of NGL components [1]

1.1.1. Economic analysis of Ethane recovery.

Figure 1 shows the difference in price for ethane and natural gas. Ethane price has always been higher than the natural gas price. Despite the later fall in price due to the increase in the conventional drilling and production technologies of natural gas liquids,

many gas processors still find NGLs economic to recover because the 2014 price is higher than that in 2013. In order for ethane prices to increase again, the demand should continue to increase in the future (as predicted by Figure 2). This analysis can be extended to NGL as it is composed mainly of ethane [1, 3].

Figure 1: Ethane price vs. natural gas price from 2005 to 2014 [3]

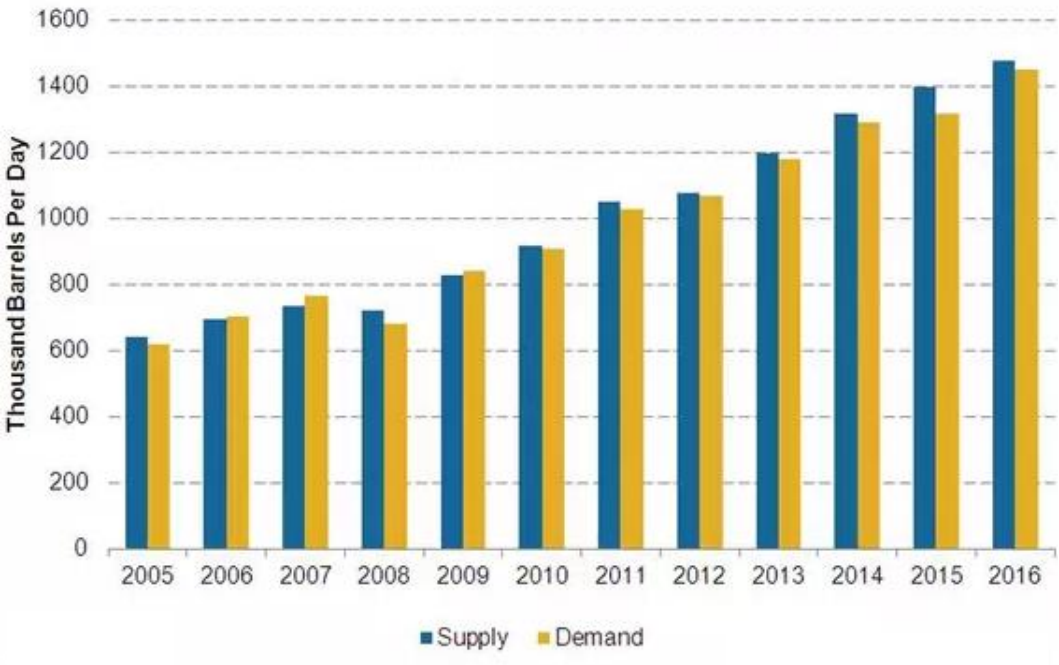

Figure 2: Ethane supply and demand from the petrochemical industry (US) [3]

1.2. Literature Review

1.2.1. NGL recovery processes.

Different processes are used to recover Ethane and heavier hydrocarbons. In this section, an overview the most common ones is provided. The first process is the mechanical (or external) refrigeration. In this process, propane is usually used as a refrigerant where it goes through a vapor compression refrigeration cycle. Second process is the Joule Thompson throttling valve also known as self-refrigeration which is favored when the wellhead pressure is high enough, so that no additional recompression will be required later on. It is an isenthalpic process and it is considered to be an energy wasting process. Third process is the Turbo expansion process in which the entering gas expands, supplying the work required for the turbine shafts and reducing the gas enthalpy. Hence, it reduces the temperature much more than the J-T throttler. Typically, turboexpantion is used in combination with refrigeration and JT expansion. Some turboexpansion processes will be discussed in the next section. Last process is the oil absorption where the absorber acts as a mass-transfer agent that dissolves NGL with a small pressure drop in the range of 5-10 psia. After that, methane will be removed and the rich oil will be separated from the NGLs in a later step. This process requires complex separation in order to remove dissolved methane from the absorber oil and it is expensive in terms of fuel requirements [2].

1.2.2. Old generation of turboexpansion processes.

Turboexpander process is the leading process for Ethane recovery [4]. Basically, it is based on expansion which is a Polytropic process that has a high reliability factor because of the simplicity of the expander/compressor combination [5]. The simple process consists of turboexpansion only, but other schemes were presented in [6]. These schemes considered the use of refrigeration, side reboilers, cold liquid exchangers and two stages of expansion. It was found that the combination of turboexpansion and refrigeration processes lower the horsepower required for a given recovery. Additionally, using the inlet gas to reboil the demethanizer reduces some of the refrigeration duty needed. With respect to the cold liquid exchanger, the liquid from the higher pressure separator is expanded and used to cool the feed. Firstly, two-stage expansion was employed for feed gases at very high pressure, but later they were used

to increase the recovery. The previous schemes could improve the accuracy of the design, choice of materials, flexibility of operation with different feed compositions, thermodynamic efficiency and profit opportunities [6]. In addition, turboexpansion processes are favored because they allow the NGL processing company from switching between ethane rejection and ethane recovery; in accordance to the cyclic ethane liquid market [7]. McKEE stated that the use of complicated schemes yields more thermodynamically efficient plant with higher ethane recovery [6]. Later on, this additional complexity in schemes was found to yield the same or less ethane recovery in some cases [8].

In the following sections, the conventional turboexpansion process is emphasized along with a few other ethane recovery processes from the new generation of NGL recovery processes.

1.2.3. Conventional turboexpander process (ISS).

In a conventional turboexpander process (Figure 3), the feed stream to the process is first cooled by providing the reboiler's duty; this might not be possible in case of high pressure in the demethanizer, where the temperature profile in the whole column is shifted up. After heat exchange with the reboiler, the feed is further cooled by heat exchange with the demethanizer's overhead in a gas-to-gas heat exchanger. Then, it is cooled in a propane chiller, hence reducing the feed's temperature to -31°F. This temperature was selected based on the lowest allowable temperature in the propane chiller which is -40°F, designed to avoid air leakage into the system [2]. The cold stream leaving the propane chiller enters a flash drum where the gas is separated from the liquid. The liquid leaving the separator is expanded and sent to the demethanizer at a lower stage than the feed. The gas outlet from the separator enters a second gas-to-gas heat exchanger for additional cooling by the demethanizer's overhead. In fact, a major constraint is to prevent the temperature cross between the two heat exchangers. Subsequently, the cooled gas leaving the second heat exchanger enters a cold separator where the liquid outlet is throttled and sent to the demethanizer at an intermediate stage. The gas outlet from the cold separator is sent to a turboexpander then to the demethanizer at a higher stage than the other two throttled streams. Part of the power required for recompressing methane emerging from the demethanizer's overhead is provided by the turboexpander [4].

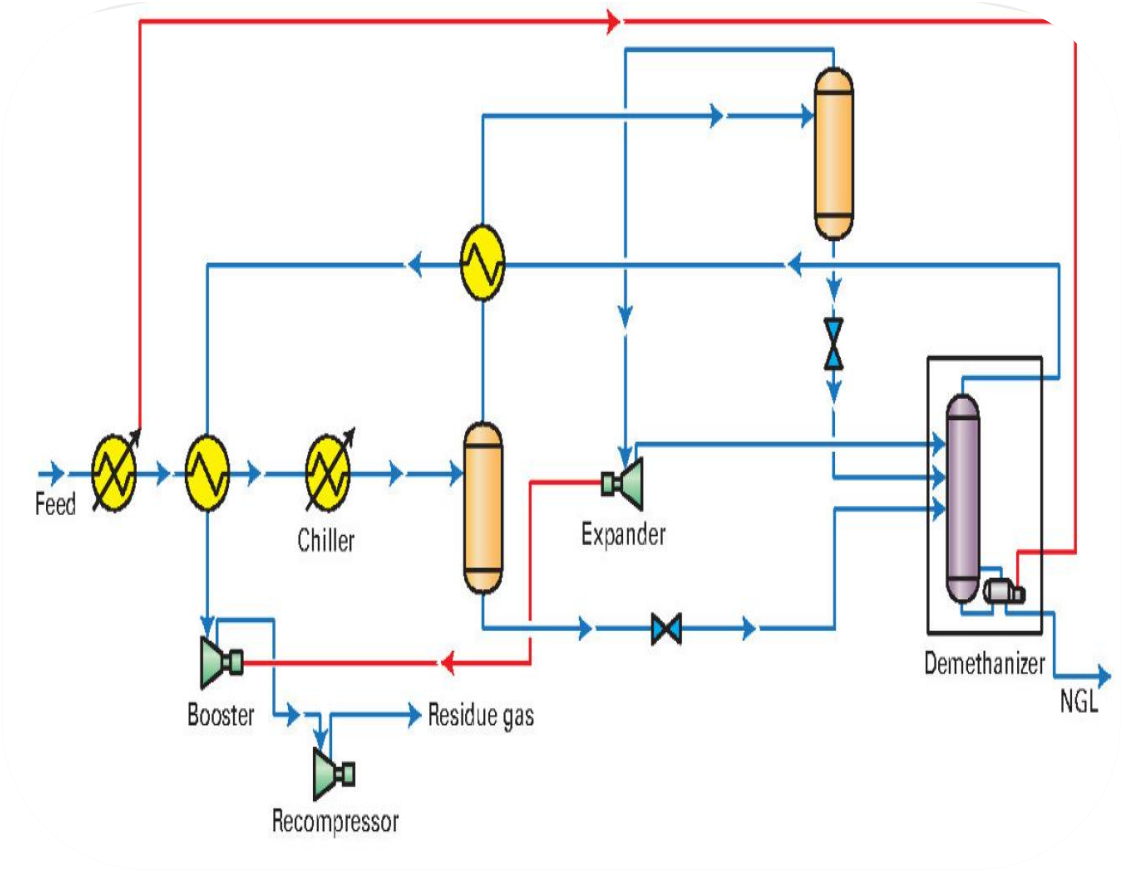

Figure 3: PFD for a conventional turboexpander process [14]

1.2.4. Warm residue recycle process (WRR or RR).

This process is similar to the conventional turboexpander process where it focuses on improving the reflux stream to the demethanizer. As shown in Figure 4, a portion of the residue gas is compressed, cooled in two gas-to-gas heat exchangers and then flashed in a throttler and sent to the top of the demethanizer as a reflux [9]. This lean cold reflux will rectify the remaining ethane in the up-flowing vapor; thus, improving ethane recovery. Moreover, this scheme reduces the capital cost by eliminating the need for a separate cryogenic compressor for the reflux as in the CRR process (discussed later in Section 2.4). However, the cryogenic compressor might be necessary if the residue gas is at a low pressure that is insufficient for liquefying the overhead vapor or when a certain pressure is optimal for achieving a very high ethane recovery [7]. The cooled inlet gas is sent to a cold separator with its gas outlet stream expanded in a turboexpander and sent to the demethanizer. The liquid outlet from the cold separator is throttled and sent to the demethanizer at a lower stage than the

previously mentioned ones. This process is CO_2 tolerant. Besides, the recovery of ethane in this process is adjustable just by changing the quantity of the recycled stream [10].

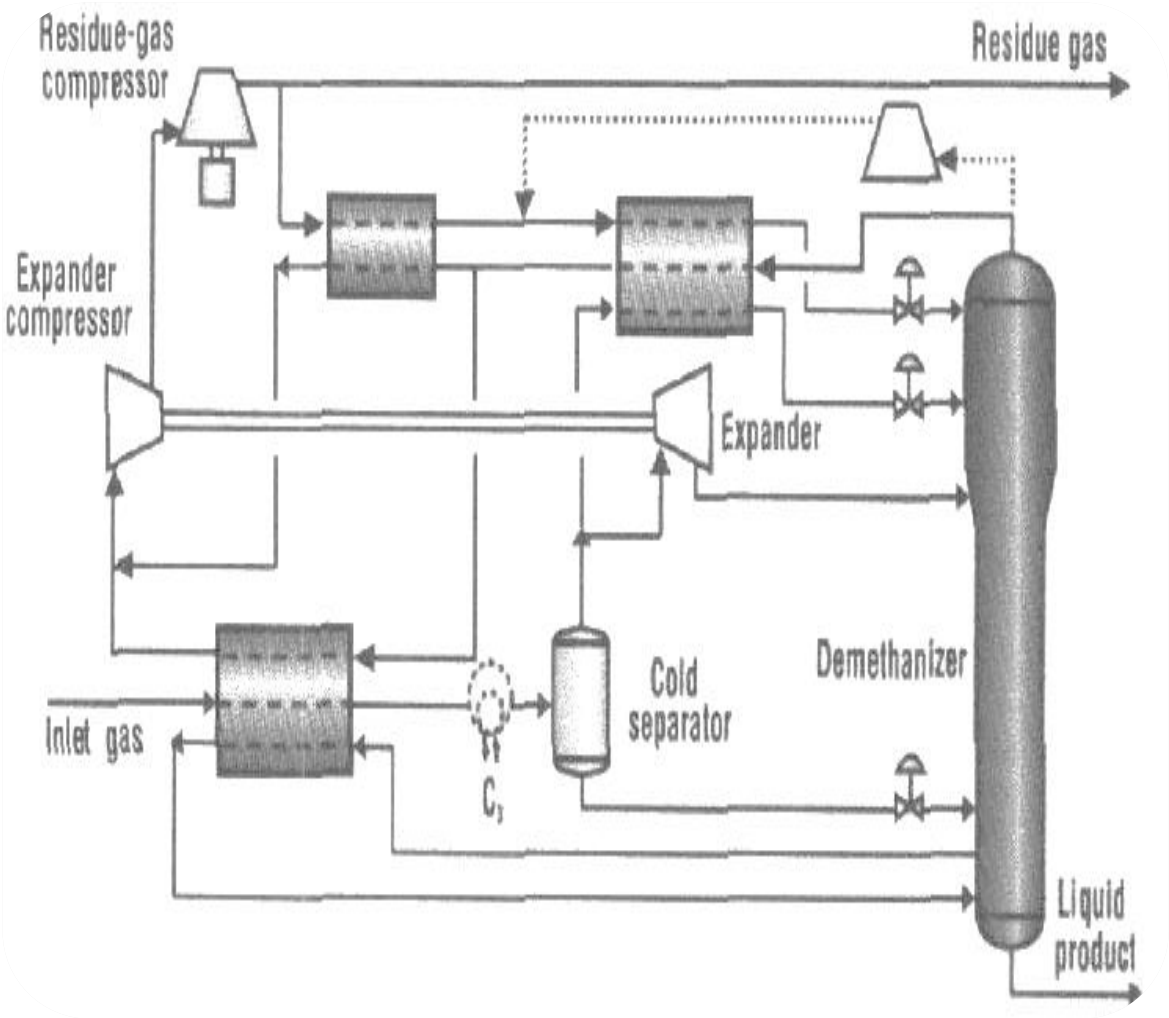

Figure 4: PFD for the RR process [7]

1.2.5. Gas subcooled process (GSP).

This process is a modified version of the conventional process with a slight change of the recycled residue portion. In this process (Figure 5), the gas emerging from the cold separator is split into two portions. One portion enters a turboexpander and then the demethanizer at an intermediate stage. The other portion is cooled with the demethanizer's overhead outlet and then, throttled before entering the demethanizer as a reflux. Because of this higher and colder reflux flow, ethane recovery is improved at

any pressure level [7]. The demethanizer's overhead is recompressed to meet the pipeline's pressure. Part of the duty required for the recompression is recovered from the turboexpander. The liquid that leaves the separator undergoes expansion in a J-T valve and enters the demethanizer at a lower stage than the outlet stream from the turboexpander [10, 11]. Even if the demethanizer is operated at a high pressure in order to reduce the recompression costs, ethane recovery will still be high due to the improved reflux [7].

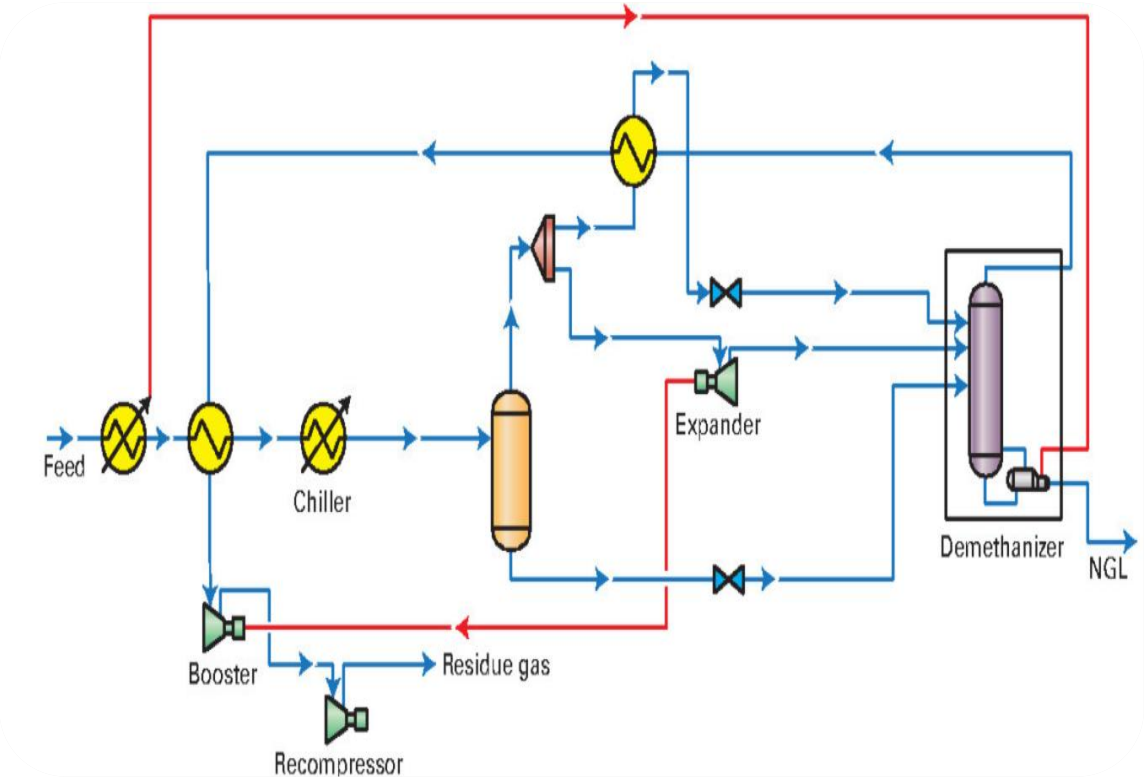

Figure 5: PFD for the GSP [14]

1.2.6. Cold residue recycle process (CRR).

The cold residue recycle (CRR) process (Figure 6) was built based on the GSP. They differ only in the demethanizer's reflux. The reflux is mainly methane, coming from the overhead stream, which is compressed to a slightly higher pressure by a cryogenic compressor, and then cooled and expanded in a J-T valve where part of the methane is condensed. The addition of the expensive cryogenic compressor could be justified by the fact that the residue stream alone is not cold enough to liquefy the slip recycle stream (as in RR process). In order to assure condensation, the stream should be at low temperature and high pressure; hence, the addition of a cryogenic compressor and

condenser [7, 12]. The residue gas is recompressed to bring the pressure up to the pipeline pressure. This process does not only provide high ethane recovery up to 98%, but also provides better CO_2 tolerance than GSP [13].

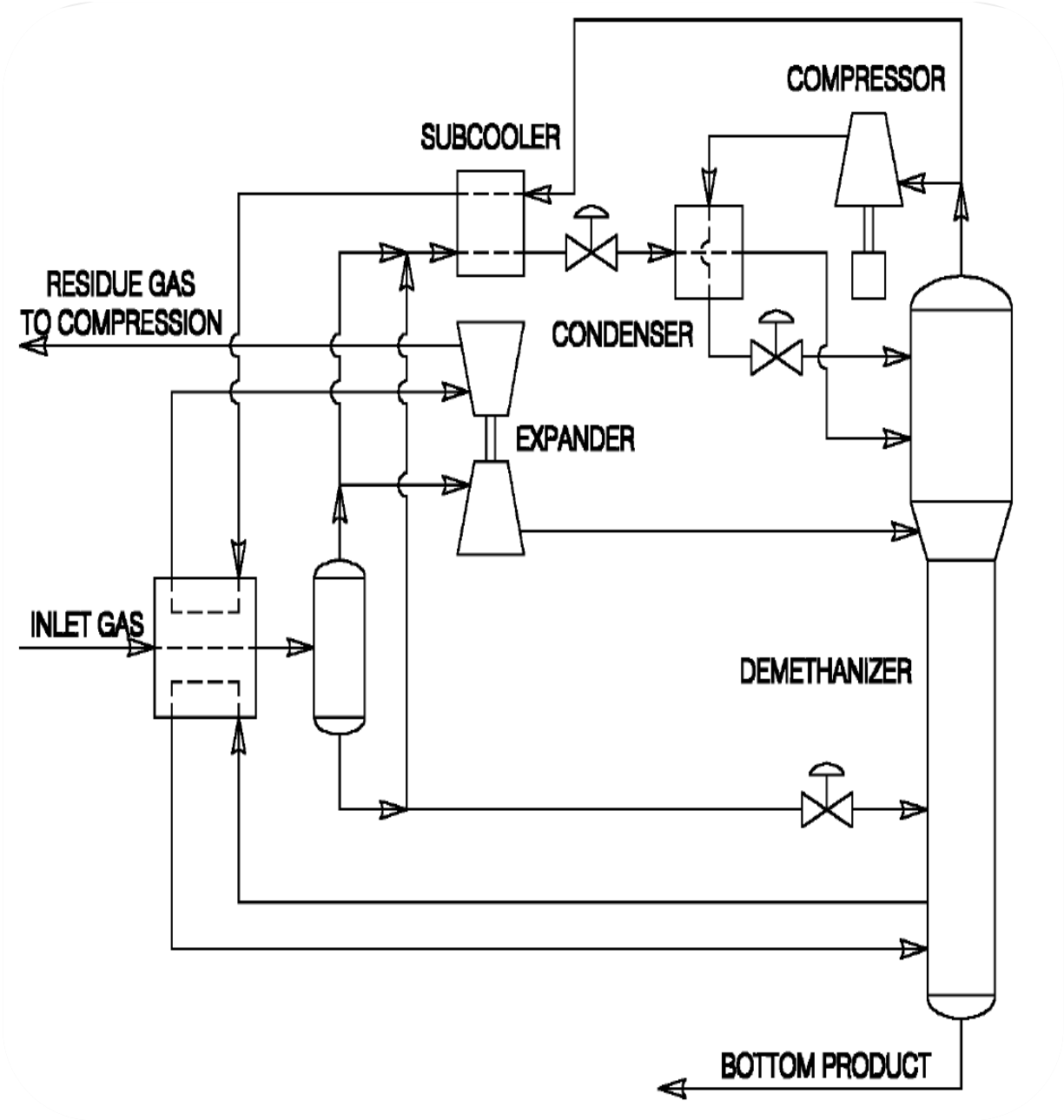

Figure 6: PFD for the CRR process [13]

1.2.7. Side draw reflux process (SDR).

The process shown in Figure 7 is another modification of the GSP where the focus is again on the improvement of the reflux stream. Here, a side stream is taken from the demethanizer where it is compressed, then cooled, sent to the condenser, and directed

to the demethanizer as a reflux. This process is beneficial when the residue gas contains inerts such as H_2. In that case, the cold separator outlet will not condense easily; however, the stream withdrawn from the demethanizer's side is inert free and can easily condense [10].

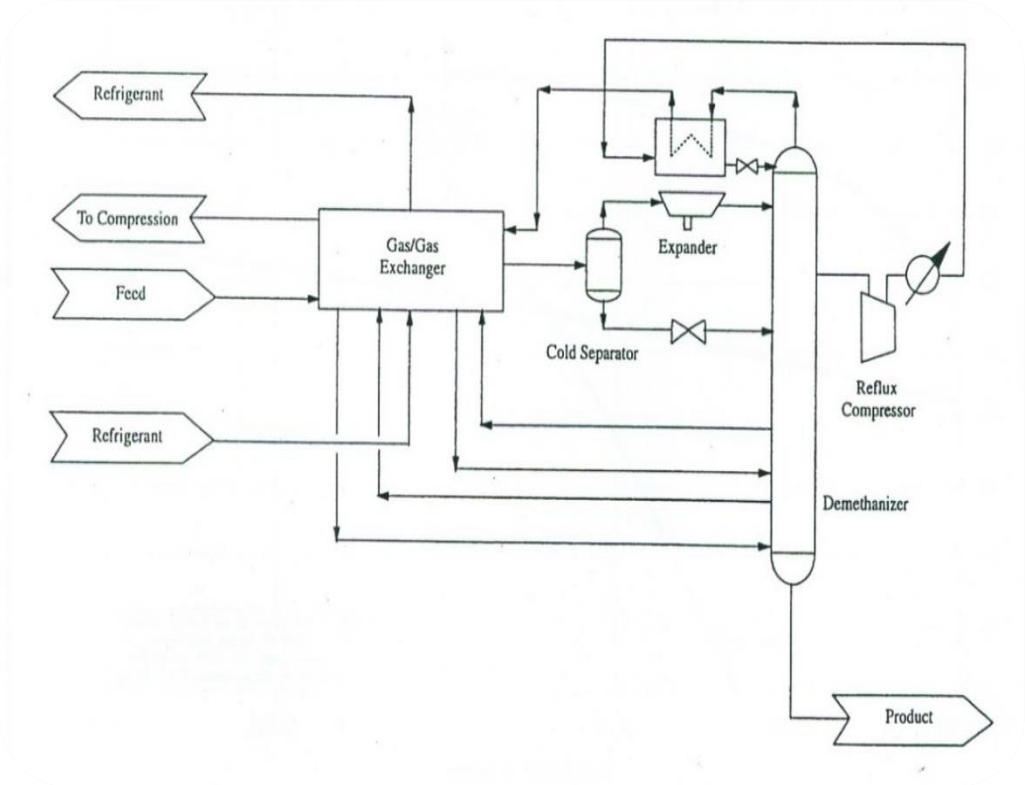

Figure 7: PFD for the SDR process [10]

1.2.8. Recycle vapor split process (RSV).

RSV, similar to the CRR, aims at improving the reflux stream. It might be better than CRR in terms of capital investment. As shown in Figure 8, a portion of the recompressed residue gas is recycled to the demethanizer after condensing and throttling it to the demethanizer's pressure. In fact, this process uses the advantages of the RR and the split vapor as in GSP. It also requires less horsepower compared to the CRR and RR processes because of two reasons. First, the presence of the split vapor lowers the reflux flow rate required to rectify the column, which is justified by the high recovery provided by the split-vapor stream [13]. Second, this process uses the residue gas

compressors for compressing the reflux stream rather than acquiring a separate compressor as in the CRR [7]. Other advantages of this process include enabling the gas processer to switch easily between the ethane recovery/rejection modes. Moreover, RSV can be operated as a GSP in case of high inlet gas flow rate just by preventing the reflux. Furthermore, this process provides better CO_2 tolerance than GSP. This is due to the higher demethanizer pressure [13].

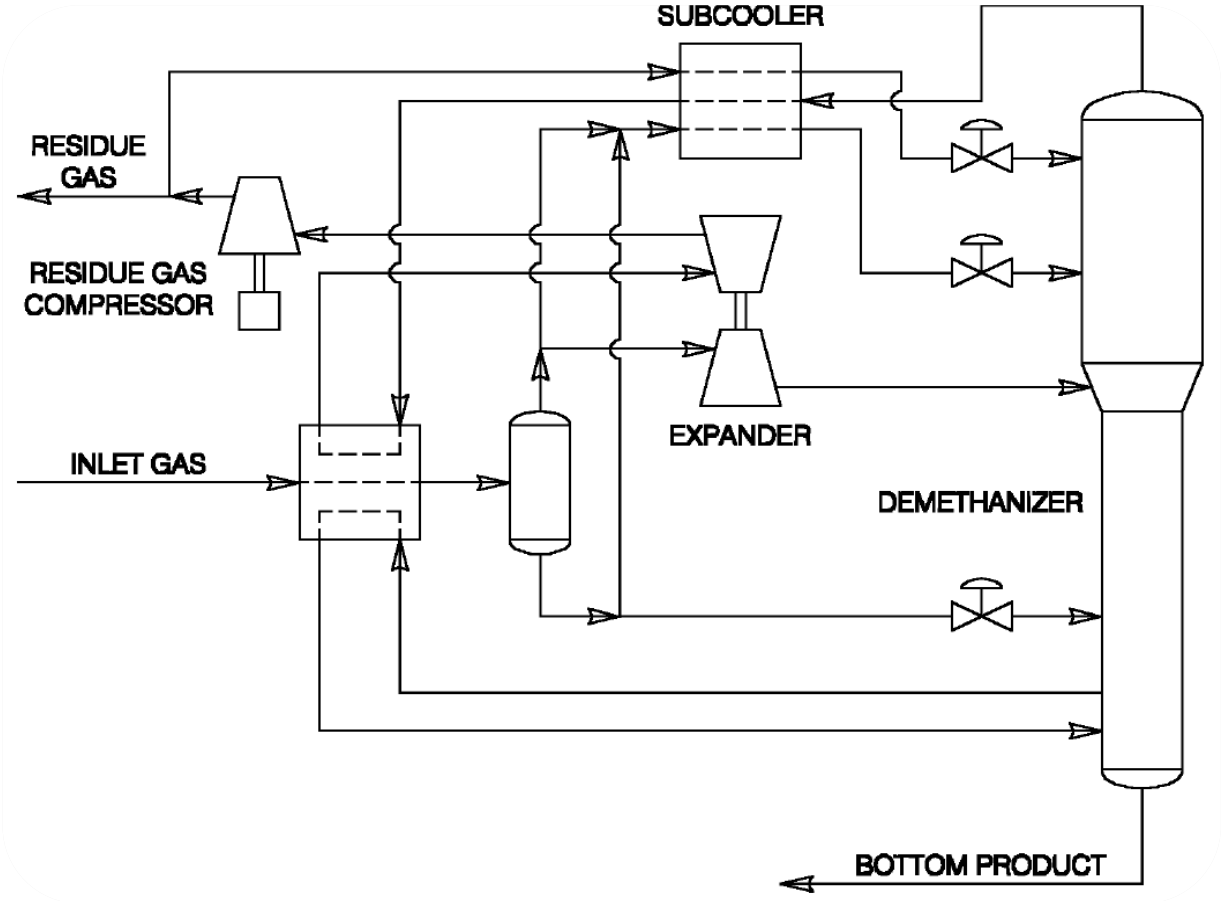

Figure 8: PFD for the RSV [13]

1.2.9. Recycle split vapor with enrichment process (RSVE).

The RSVE (Figure 9), as the name suggests, is a modification on the RSV. In this process, part of the compressed residue gas is mixed with the split-vapor feed before it condenses, which eliminates the need for a separate heat exchange passage. This results in a lower capital cost. Moreover, RSVE has a better CO_2 tolerance compared to RR and RSV. This is justified by the reflux stream which is rich in heavier hydrocarbons that increases the bubble point of the top section of the column and hence, shifting the

demethanizer's conditions away from frosting. The disadvantage of this scheme, however, is the lower ethane recovery because more ethane is present in the tower's top feed [13].

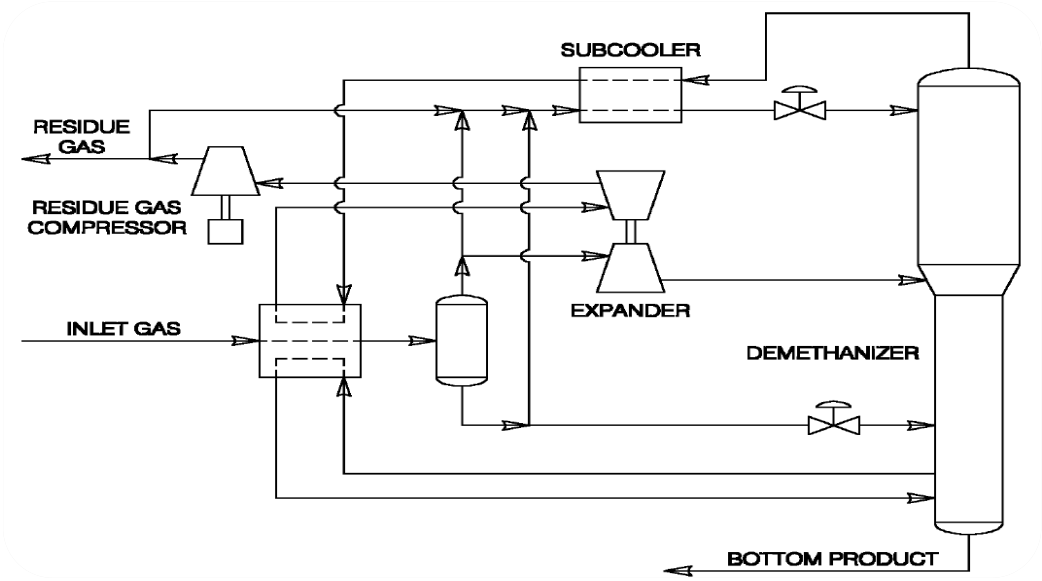

Figure 9: PFD for the RSVE process [13]

1.2.10. Liquid subcooled process (LSP).

In this process (Figure 10), the liquid from the low temperature separator is subcooled further before it is split into two streams. One stream is throttled and sent to the top of the demethanizer. The second liquid stream is throttled in a J-T valve before it enters a heat exchanger where it cools the feed to the LTS. After that, it is throttled before entering the lowest section. The vapor stream is expanded in a turboexpander before entering the intermediate section of the column. This process reduces the energy consumption. Also, the cold heavy hydrocarbon fed to the top section of the demethanizer will act as a gas scrubber [11, 15].

1.2.11. Gas liquid subcooled process (GLSP).

This process combines the advantages and disadvantages of GSP and LSP. It was found that the GLSP gives a higher average recovery compared to the GSP and the LSP, regardless of the nature of the feed [11, 15].

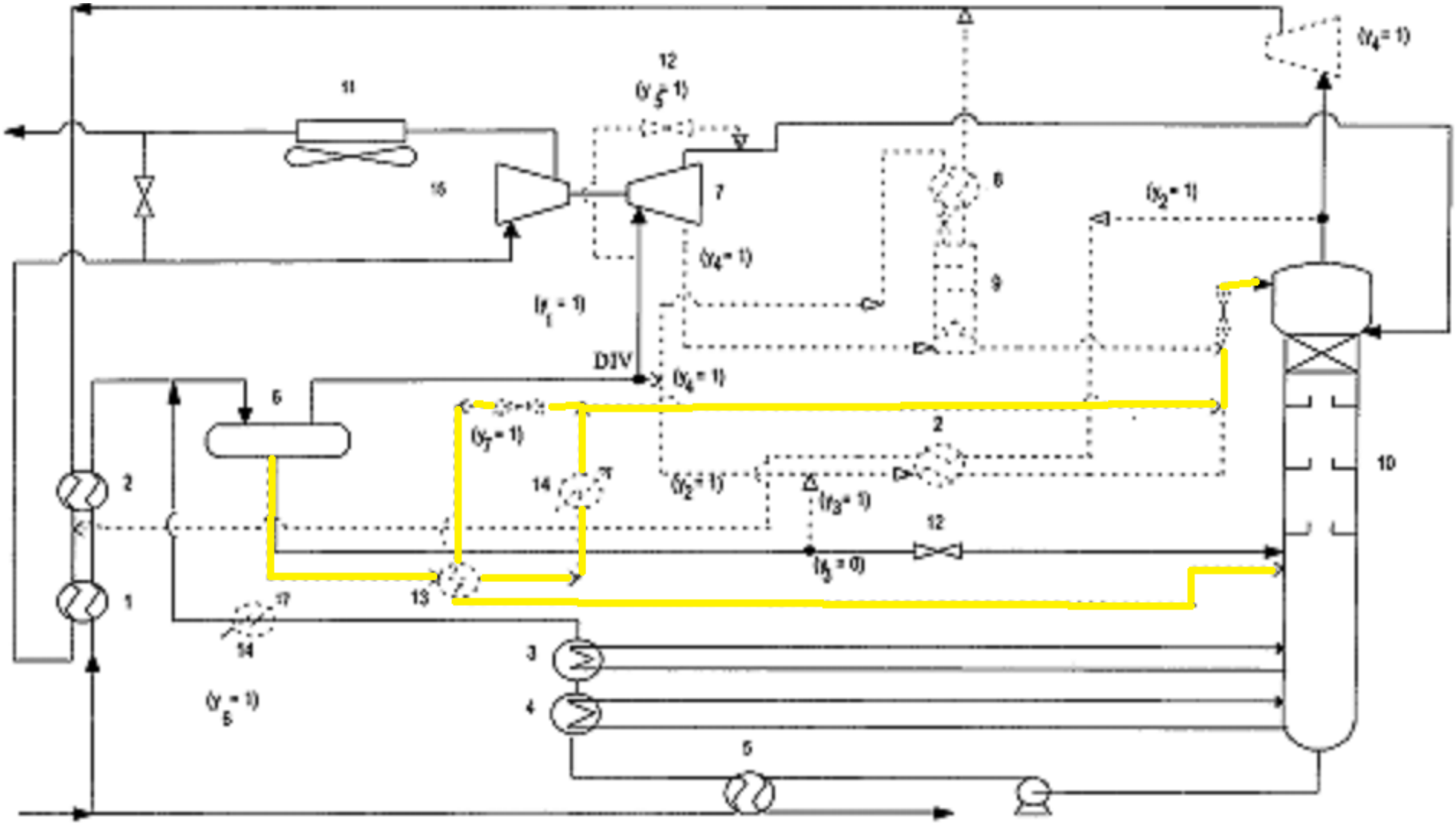

Figure 10: PFD for the LSP process [11]

1.2.12. Lean reflux process (LRP).

In this process (Figure 11), the feed gas is split into two streams. One portion is cooled by heat exchange with the residue gas in a gas-to-gas heat exchanger and the other stream provides heat duties for the reboiler and a side reboiler. Then both streams are combined and fed to the low temperature separator (LTS). The liquid from the LTS is throttled and sent to the demethanizer. The gas leaving the LTS is divided into two streams; the first is expanded in a turboexpander and fed to the middle section of the column, whereas the second is fed into a lean reflux absorber along with the demethanizer's overhead stream. The lean reflux emerging from the absorber is sent to the top of the demethanizer to enhance ethane recovery. The overhead stream that leaves the absorber is sent to a heat exchanger to cool the feed, then it is compressed as a residue gas. The absorber eliminates the need for the compression of lean gas recycled stream [7].

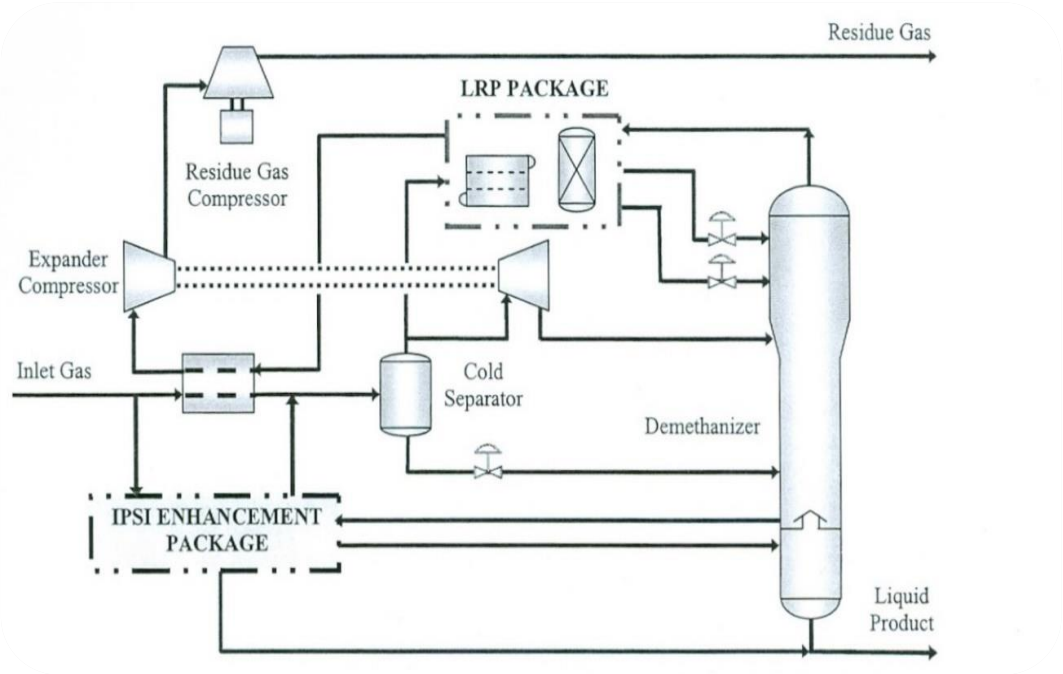

Figure 11: PFD for the LRP [7]

1.2.13. IPSI-1.

This process focuses on improving the bottom of the demethanizer column. Here (Figure 12), a stream from the bottom of the demethanizer is throttled, and used to cool the feed before it enters a separator, thus reducing or eliminating the need for refrigeration. The gas leaving the separator is expanded and sent back to the bottom of the column where it acts as a stripping gas. This stripping gas is warm enough to reduce

the reboiler duty. Moreover, it enhances the relative volatility in the column by raising the critical pressure. Lastly, it helps in reducing the temperature profile in the column which can be used for reducing the feed temperature and subsequently, reducing the refrigeration requirements [7]. The liquid leaving the separator is pumped and mixed with the demethanizer bottom product.

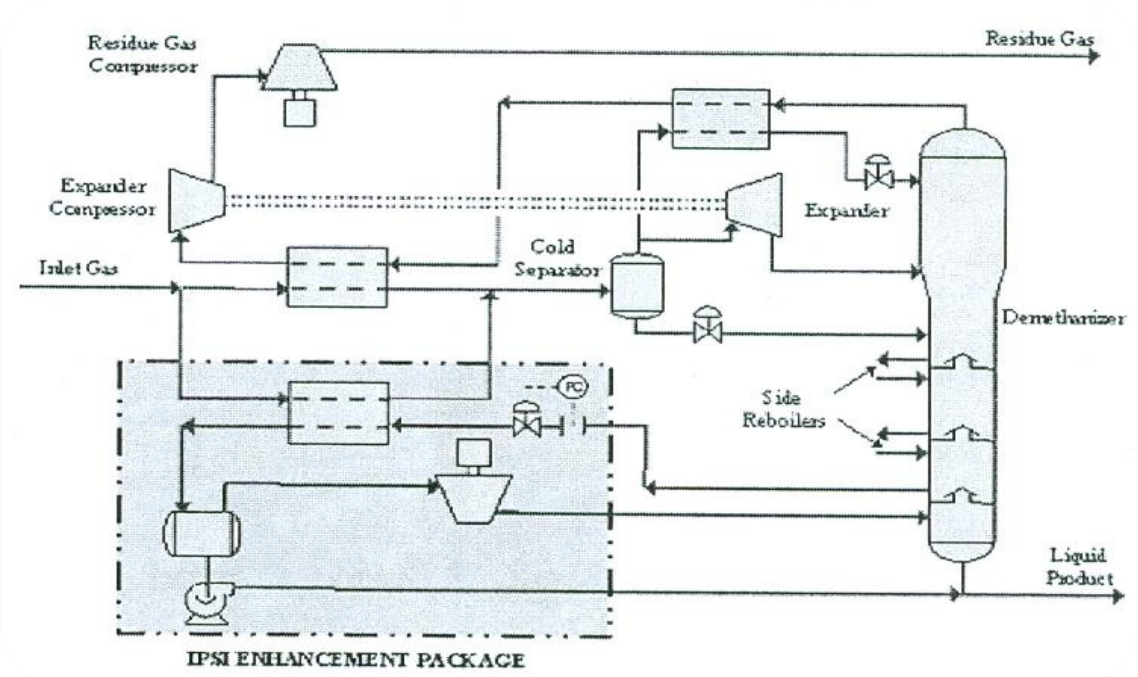

Figure 12: PFD for the IPSI-1 [7]

1.2.14. IPSI-2.

Similar to IPSI-1, this process utilizes a stream near the bottom of the column (Figure 13). This stream is used to cool the feed in two stages. The stream leaving the first heat exchanger will be throttled and then used as a refrigerant (open refrigeration cycle). The open self-refrigeration cycle eliminates the need for external refrigeration. After emerging from the heat exchanger, this stream is fed to the flash separator, where the vapor effluent is compressed, then cooled before entering another separator. A portion of the liquid stream leaving this separator is mixed with the liquid stream leaving the column to be used as a refrigerant, which represents the closed-self refrigeration cycle. This cycle eliminates the need for external refrigeration and reduces the reboiler duty as it reduces the temperature of the column [16, 17].

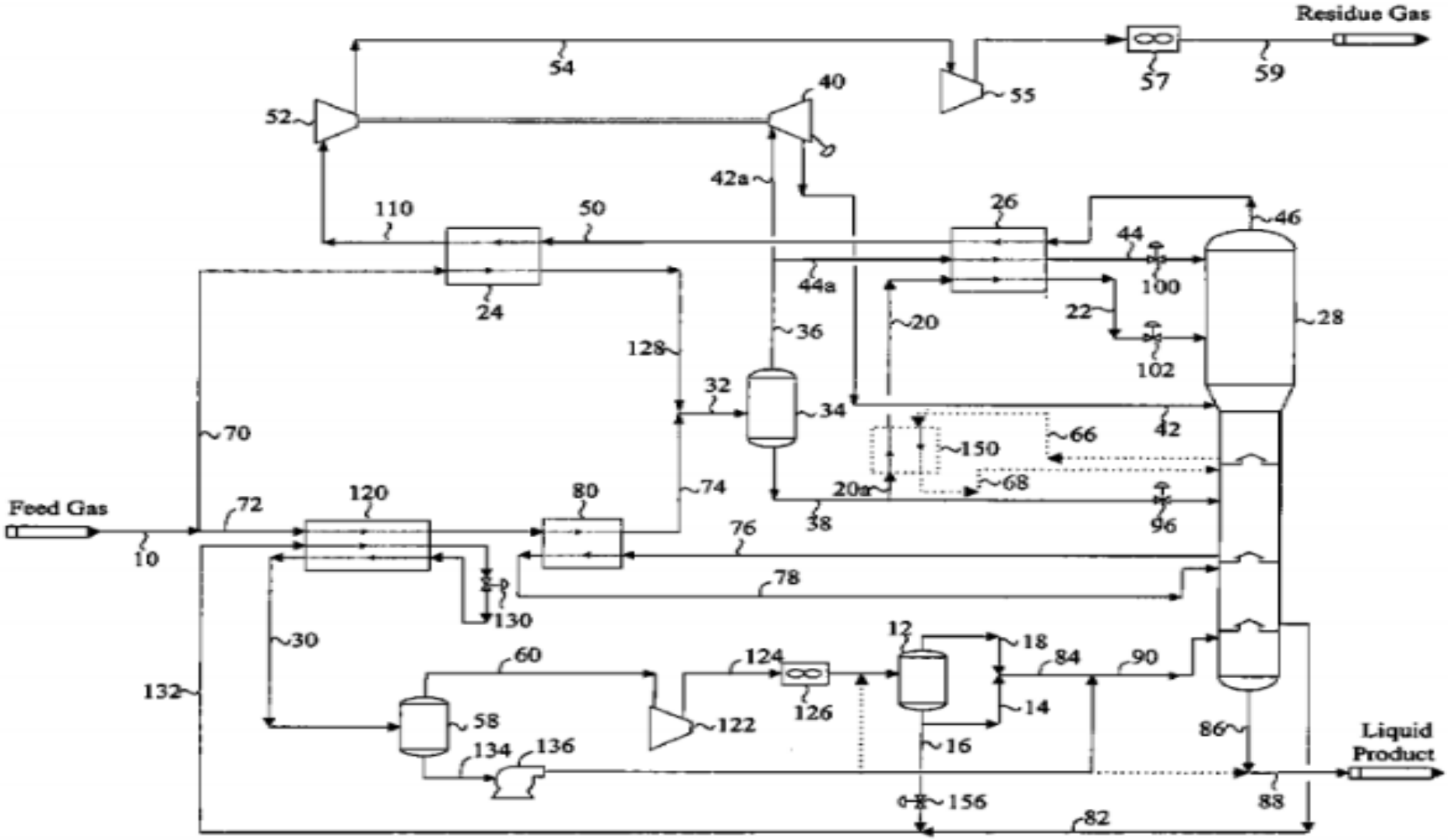

Figure 13: PFD for the IPSI-2 [16]

1.2.15. Comparison between turboexpansion processes.

The advantages and disadvantages of each turboexpansion process are listed in Table 2.

Table 2: Advantages and disadvantages of each turboexpansion process

Process	Advantages	Disadvantages
ISS	-Simple scheme	
RR	- Ethane recovery is adjustable by changing the quantity of recycled stream [10] - CO_2 tolerant [10]	
GSP	-Higher recovery than ISS [7]	
CRR	-Highest recovery up to 98% [13] -Better CO_2 tolerance than GSP [13]	-Cost of the additional cryogenic compressor [13]
SDR	-Good when the residue gas contains inerts [10]	
RSV	-Requires lower horse power than RR [13] -Requires lower reflux than the CRR [13] -Flexibility in switching between ethane recovery and rejection modes [13] -Better CO_2 tolerance than GSP [13]	
RSVE	-Better CO_2 tolerance than RR and RSV [13] -Lower capital cost [13]	-Lower ethane recovery [13]
LSP	-Lower capital cost [11, 15] -Better separation of methane [11, 15]	
GLSP	-Higher ethane recovery than GSP and LSP [11, 15]	
LRP	-Absorption eliminates the need for compressing the recycled stream [7]	
IPSI-1	-Lower reboiler duty [7] -Better separation in the column [7] -Lower temperature profile in the column [7]	
IPSI-2	-Lower need for external refrigeration [16, 17]	

1.2.16. Other related works.

Several studies on the optimization of turboexpansion ethane recovery processes are available in literature. The optimization was either based on ethane recovery or on the net profit of the process. This section includes a brief description of each of these studies.

1.2.16.1. *Optimization of ethane recovery*

Jibril et al. [15] compared ethane recovery of ISS, GSP, LSP and GLSP for a wide range of feed compositions. They found that the GLSP yielded the highest recovery at various feed compositions. Moreover, it was shown that the GSP yielded the highest recovery in the case of medium C_{2+} composition. Furthermore, the composition of C_{2+} in the feed was found to determine which cryogenic process should be used.

Pitman and Hudson [13] studied the performance of GSP, CRR, RSV, and RSVE for certain gas streams operated at ethane recovery/ethane rejection modes based on the relative compression power. When compared to the GSP, the new processing schemes gave a higher recovery at a certain compression power.

Kherbek and Chebbi [12] considered ethane recovery in GSP and CRR processes. They found that the optimized CRR process reduces to the GSP for all feeds and demethanizer pressures except for the lean feed at low demethanizer pressure where the CRR process yields higher ethane recovery.

Mazroui et al. [14] compared ethane recovery in the GSP and ISS processes for a variety of feed compositions and pressures. It was found that decreasing the demethanizer pressure increases ethane recovery for all of the feeds considered. In case of lean feed gas at low demethanizer pressure, the GSP gives higher ethane recovery while the conventional turboexpantion process yields a higher or equal ethane recovery in all of the other cases.

Lee et al. [7] compared ethane recovery in GSP, GSP+, CRR, WRR and LRP processes. It was found that the CRR and the LRP give the highest ethane recoveries with close recovery values for the GSP+ and the WRR. Moreover, the compression requirements for all processes were compared. The GSP requires the highest compression while LRP needs the lowest.

Chebbi et al. [8] simulated five ethane-recovery processes. It was found that additional complexity might not increase the ethane recovery in some cases. Moreover, it was shown that processes with a reflux stream have a lower ethane recovery. Higher ethane recoveries were associated with turboexpander processes that use gas-gas and gas-liquid heat exchanger and utilize part of the feed to provide the reboiler duty.

1.2.16.2. *Optimization of Profit*

Getu et al. [17] performed an economical assessment of the ISS, GSP, CRR, RSV, IPSI-1 and IPSI-2 processes with common operating criteria. A comparison between all processes was held based on the capital cost, the operating cost and profitability analysis. They considered lean and rich gases. It was found that IPSI-1 has the best economic performance for both feeds.

Chebbi et al. [4] optimized the profit in conventional turboexpander process under different demethanizer pressures and different feeds (lean and rich). The analysis included the refrigeration loop. Optimal ethane recovery for each demethanizer process was compared with the maximum possible value at the same pressure. It was concluded that in most of the cases, the maximum recovery corresponds to the optimum profit at a given demethanizer pressure.

Mehrpooya et al. [18] investigated the cost analysis for different turboexpansion processes including the refrigeration loop. The optimization was performed using advanced genetic algorithm program. The best process was the turboexpander-exchange process in which the profit increased by 28%.

Diaz et al. [11] compared the profit using the following processes: GSP, LSP, BTEB (basic turboexpander process) and the 2-sDP (two-stage demethanizer process) for different feed compositions. GSP was found to yield the highest recovery for most of the feeds. Optimization was performed using mixed integer non-linear programming (MINLP). It was found that as the CO_2 content increases, ethane recovery decreases.

Mehrpooya et al. [19] simulated and optimized an ethane recovery plant and compared the results with the original plant data. They implemented Shuffled Frog Leaping algorithm for the optimization of the plant profit. It was found that the process and the refrigeration cycle configurations could be improved to provide higher profit.

1.3. Problem Statement

Despite the high interest in turboexpansion processes for NGL recovery, most researches in this area were developed to maximize the recovery of certain NGLs without providing a comprehensive economic justification for the processes encountered. In literature, most processes target the recovery of ethane because if ethane was successfully recovered, the remaining NGLs are less volatile and easier to recover. The specifications of the input to the process along with the process constraints and products are specified. The objective function is cost oriented and related to maximizing the profit of the process as in Chebbi et al. [4] based on the formulation in Turton et al. [6]. The objectives of this work are to:

- Optimize CRR and GSP turboexpansion processes to check whether the high ethane recoveries obtained by the CRR scheme provide a higher profit
- Use sensitivity analysis to determine the effect of each design variable on the objective function
- Optimize processes for different feed compositions
- Optimize the processes at three typical demethanizer pressures (100, 215 and 450)
- Check the necessity of external refrigeration
- Check the effect of CO_2 content on the results. The effect of CO_2 is important because turboexpansion processes are operated at cryogenic temperatures below -70 °F which leads to the formation of solid carbon dioxide (CO_2 frost point) at sufficiently high CO_2 content [2]

1.4. Scope of the Present Work

In the present work, the Cold Residue Recycle (CRR) process is considered for NGL recovery. The selection of the process is based on the claim that the CRR process yields a very high ethane recovery that can reach up to 99.8% [12]. CRR process is simulated at a low demethanizer pressure (100 psia). Each unit in the process is then sized based on some heuristics in chemical engineering. Then, the bare module cost of each unit in the process is evaluated based on the size attribute. Sensitivity analysis is performed to investigate the effect of each of the design variables on the objective function. Finally, optimization is done to obtain the best operating conditions that

maximize the objective function. The CO_2 effect on CRR and GSP is demonstrated at a demethanizer pressure of 100 psia.

Chapter 2. Simulation

2.1. CRR Process Simulation

The simulation of the CRR process (Figure 14) was performed on Aspen HYSYS using the Peng-Robinson equation of state. The pressure, temperature, and flow rate of the feed stream are kept constant at 882 psia, 100 °F, and 10,980 lbmol/h, respectively. The residue gas is compressed to 882 psia in order to meet the sales gas requirements. In order to stabilize the liquid product, the molar ratio of methane to ethane in the bottom product of the demethanizer is fixed at 0.02 as in common practices [2].

Following is the process description of the base case for a demethanizer operated at 100 psi pressure. The natural gas feed stream enters heat exchanger (E-100) where it is cooled by providing the duty of the reboiler. The feed is cooled further by exchanging heat with the demethanizer's overhead product in exchanger E-102 at very low temperatures. Then, the feed is cooled further using external refrigeration cycle as will be illustrated in Section 2.2. The chilled gas leaving the refrigeration cycle enters vessel V-100 where it is flashed into gas and liquid streams at -31°F. The gas stream that leaves the cold separator is devided into two portions. One portion of the gas stream enters a turboexpander K-104 and then a demethanizer T-100 at an intermediate stage. The liquid stream leaving the vessel is also divided into two parts. The first part of the liquid stream is mixed with the part of gas stream 8 before entering the demethanizer. The other portion of the liquid is throttled before entering the demethanizer at a lower stage than the outlet stream from the turboexpander. Part of the residue gas is compressed in K-100, cooled, throttled and sent back to the column as a reflux. The part of the residue gas used to cool the feed is finally compressed in booster K-101 then in a two-compression system (K-102 and K-103). Part of the recompression duty is recovered from the turboexpander and the other part is obtained by burning part of the residue gas using a gas turbine as a drive.

The process flow diagram of the CRR differs for other demethanizer pressure such as: 215 and 450 psi. These differences include the external heat source requirement, the different refrigeration requirements, and the recompression duty differences. The different demethanizer conditions are explained in details in Chapter 4.

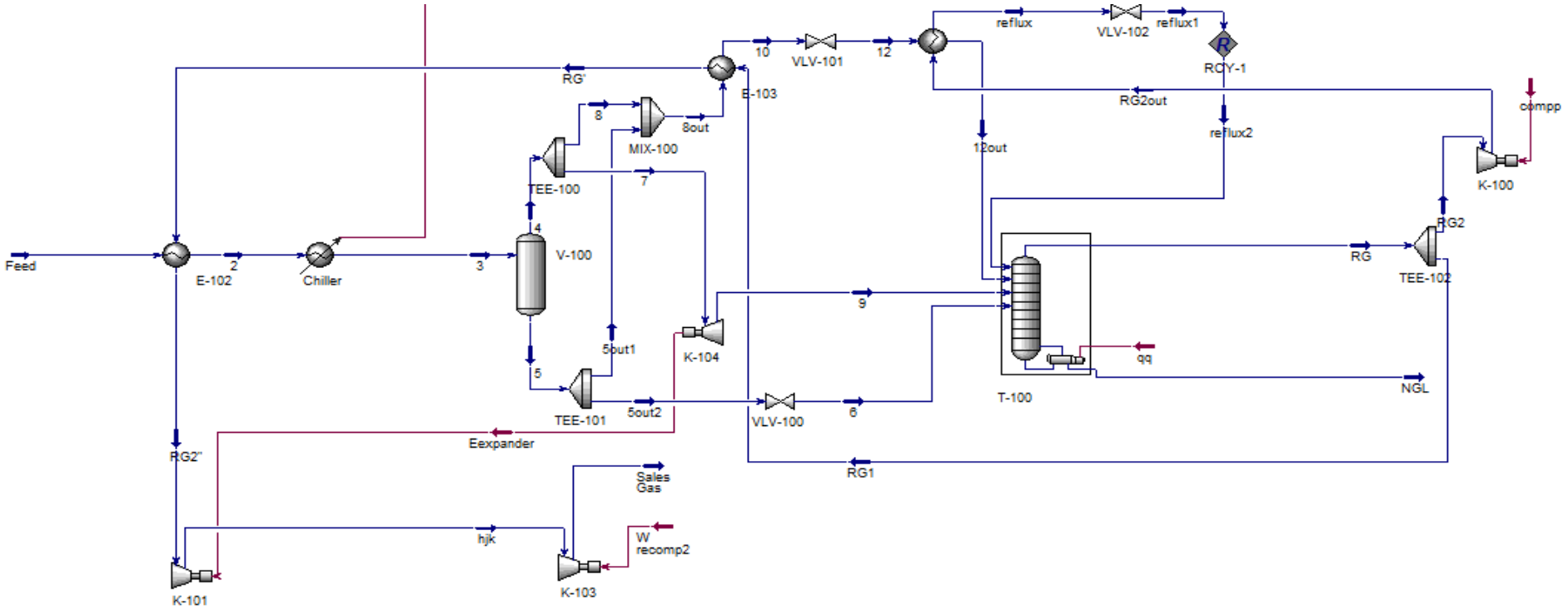

Equipment (s)	Description	Equipment (s)	Description	Equipment (s)	Description	Equipment (s)	Description
TEE-100,101,102	Splitter	K-100,101,102,103	Compressor	T-100	Demethanizer	VLV-100,101,102	Valve
E-100	Cooler	K-104	Expander	V-101	Vessel		
E-102,103,104	Heat Exchanger	MIX-100	Mixer				

Figure 14: CRR process flow diagram

2.2. Refrigeration Cycle

Propane economizer cycle (Figure 15) was used because it requires less recompression power than the propane refrigeration simple cycle. The saturated liquid leaving the storage tank is flashed to an intermediate pressure, also known as economizer pressure. The effluent from the condenser is flashed in the economizer flash drum, where the vapor from the drum is separated from the liquid and compressed afterwards in the second stage of compression. The liquid from the drum is flashed from the economizer pressure to the chiller's pressure, consequently producing a lower amount of vapor relative to the simple cycle. The vapor leaving the chiller is compressed to the economizer pressure before being mixed with the economizer vapor. The mixed stream is compressed to the condenser's inlet pressure [2].

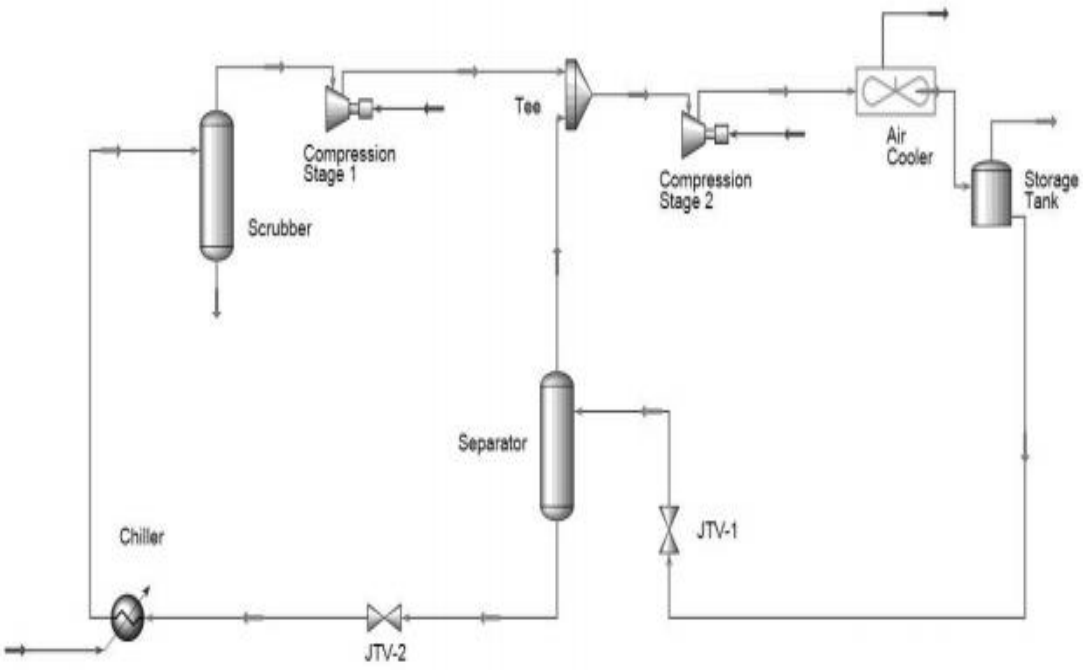

Figure 15: Economizer refrigeration cycle

2.3. Feed Composition

The composition of the feed varies between rich and lean (Table 3). The classification of the feed stream as lean and rich is based on the C_2^+ content. The feed is considered lean if it contains less than 2.5 GPM C_2^+. If the feed contained more than 5 GPM, it is considered rich [2]. The refrigeration energy requirement for the rich feed

is higher than that of the lean feed because of the cost associated with condensing the heavier hydrocarbon in the rich feed. As the content of the heavier hydrocarbon increases in the feed stream, the demethanizer reboiler will require more energy to operate.

Table 3: Feed stream molar composition

Component	A	D
Nitrogen	0.01	0.01
CO_2	0.00	0.00
Methane	0.93	0.69
Ethane	0.03	0.15
Propane	0.015	0.075
Butanes	0.009	0.045
Pentanes	0.003	0.015
Hexanes	0.003	0.015

Table 4: Feed stream content of heavy hydrocarbons

Content	A	D
% C_2^+	6	30
GPM	1.72	8.6

2.4. Demethanizer

The ideal operation of the demethanzier column was assumed. One can predict that the vapor leaving the column will contain all of the methane and no heavier hydrocarbons. The heavier hydrocarbons should ideally leave with the bottoms stream [9].

The demethanizer column was designed as a trayed fractionator as found in most of the gas processing plants. Sieve trays in particular were used due to their efficiency, low cost, ease of maintenance and operability [20]. The overall tray efficiency ranges between 40 and 50 [21]. The column was simulated on HYSYS simulator as a reboiled absorber. Initially, the locations of the feed streams were selected to match the

temperature and composition profiles in the column with the temperatures and compositions of the feed streams.

The deethanizer typically operates at a pressure between 100 and 450 psia [13]. Part of the residue gas leaving the demethanizer is recycled back as a reflux to the top of the demethanizer, as described in Section 2. At low and intermediate demethanizer pressures (100 and 215 psia), the feed is partially cooled by providing the reboiler's duty. However, at high pressure (450 psia), the temperature profile of the column is shifted up due to the high pressure. Hence, the temperature of the feed is not hot enough to provide the reboiler duty. Thus, an external heating source, namely low pressure steam, was used to provide the heat. Kettle reboiler is commonly used in the demethanizer design. Moreover, the relative volatility decreases with the pressure which makes the separation of the key components harder.

2.5. Compressors and Expanders

Most of the compressors used in the main process are centrifugal. The only compressor that was selected differently is the overhead compressor in the CRR, which was designed as a rotary compressor due to its small size.

Part of the power required for the recompression is provided by the turboexpander. Other compressors are driven by heat engines/gas turbines that are operated using part of the sales gas. Operating the demethanizer at low pressure allows for more expansion across the tuboexpander, which leads to a lower process temperature and more NGL recovery. However, larger sales gas compressors will be required.

2.6. Heat Exchangers

Heat exchangers (E 100, E 101 and E 102) are used to pre-cool the feed stream to the process. E 103 is used to further cool stream (12out), fed to the third stage of the demethainzer. E 104 is used to cool stream (reflux2) to the lowest possible temperature before entering the first stage of the demethanizer. All of the heat exchangers used in the study are gas-to-gas exchangers of shell and tube type. Countercurrent flow is used in all heat exchangers to achieve more efficient heat transfer. The heat exchanger was simulated using type "E" shell that consists of one-pass shell.

2.7. Process Vessels

The gas-liquid separators are designed as vertically-oriented vessels with a demister pad. The configuration of the vessel was selected based on the low gas-to-liquid ratio found in the simulation [22]. V-100 is operated at -31 °F and 882 psia where liquid hydrocarbon is firstly separated from the gaseous components.

2.8. Material of Construction

Due to the low temperatures expected in an NGL recovery process, the selection of the materials of construction was based on the following criteria:

- Carbon steel is used in all equipment wherever the temperature is above -40 °F [2]
- The selection of carbon steel is cost based. Nickel alloy and stainless steel are much more expensive than carbon steel. The industrial practice is to use carbon steel in all equipment as long as it is safe and reliable
- If, on the other hand, the design temperature was below -40 °F, carbon steel becomes brittle, hence, stainless steel is used instead [2]
- The demethanizer, trays, overhead compressor, upper heat exchnagers (HE-103 and HE-104) and the tube side of heat exchanger HE-102 are operated at low temperatures. The aforementioned equipment are made of stainless steel
- HE-102 was designed to place the more corrosive fluid in the tube side in order to reduce the stainless steel usage in the shell side or in the cladding.

Chapter 3. Cost Model

3.1. Cost Model Approach

In order to evaluate the objective function that is related to the profit, the CRR process is simulated using HYSYS simulator. After simulating and evaluating the objective function for a base case, sensitivity analysis is performed to determine the primary design variables. Next, optimization is performed to maximize the objective function and obtain the corresponding operating conditions.

3.2. Objective Function

The objective function is related to the annual profit of the plant [23]. The profit can be calculated by:

$$\text{Profit} = \text{SG} + \text{SNGL} - \text{C}_{\text{RM}} - \text{COM}_{\text{d}} \quad (1)$$

and the cost of manufacturing without deprecation is given by [23]:

$$\text{COM}_{\text{d}} = 0.180\ \text{FCI} + 2.73\ \text{C}_{\text{OL}} + 1.23\ (\text{C}_{\text{UT}} + \text{C}_{\text{WT}} + \text{C}_{\text{RM}}) \quad (2)$$

where SG = residue gas Sales, $/yr

SNGL = NGL sales, $/yr

C_{RM} = cost of raw material, $/yr

COM_{d} = cost of processing without depreciation, $/yr

C_{OL} = cost of operating labor, $/yr

C_{WT} = cost of water treatment, $/yr

The multiplication factors in Eq.3 are obtained by adding the midpoint values of each term that appear in three cost categories, namely: direct manufacturing costs, fixed manufacturing costs and general manufacturing expenses [23]. The costs of the operating labor and the feed gas are constants. Also, there are no water treatment facilities in the process.

Hence, Eq.1 reduces to Eq.3:

Objective function (B) $= SG + SNGL - 0.180FCI - 1.23C_{utility}$ (3)

3.3. Design Variables

Six design variables were considered in the optimization of the CRR process where the subscripts denote the name of the stream. These variables are:

1. T_{10} : Temperature of the gas stream leaving the separator after exchanging heat in E-103
2. T_{12out} : Temperature of the split vapor feed to the demethanizer
3. P_{RG2out}: Pressure at the outlet of the cryogenic compressor
4. $\dot{M}_8$: Molar flow rate of stream 8
5. $\dot{M}_{5out2}$: Molar flow rate of stream 5out2
6. $\dot{M}_{RG2}$: Molar flow rate of stream RG2

The same variables are also used for the optimization of the GSP except that for the GSP the cryogenic compressor K-100, heat exchanger E-104 and splitter TEE-102 do not exist. In that case, the following three design variables are discarded:

T_{12out} : Temperature of the split vapor feed to the demethanizer

P_{RG}: Pressure at the outlet of the cryogenic compressor

$\dot{M}_{RG2out}$: Molar flow rate of stream RG2

If external refrigeration is required, two additional design variables are included:

7. T_2 : Temperature of the inlet stream to the chiller
8. P_{econ}: Economizer pressure

3.4. Constraints

The constraints were selected in order to prevent temperature cross in the heat exchangers, assure that the temperature of the split vapor feed to the demethanizer is lower than the reflux temperature, and ensure that the recycle loop is converging. The constraints are:

1. $T_2 > T_{RG2}$"
2. $T_3 > T_{RG}$"

3.$T_{10} > T_{RG'}$

4.$T_{12out} > T_9$

5.$T_{12out} > T_{reflux2}$

6.$T_{reflux1} = T_{reflux2}$

3.5. Sensitivity Analysis

3.5.1. Background.

A sensitivity analysis was performed to check the effect of each design variable on the objective function for each case. The sensitivity analysis presented in this section is specific for the case of lean feed at 100 psia demethainzer pressure and low NGL/gas price ratio. The same analysis was carried over for each case. In case of lean gas at 100 psia, self-refrigeration is sufficient to provide the required refrigeration duty as will be discussed in Chapter 4. Thus, the optimization variables related to the external refrigeration loop are discarded.

It is also important to mention that the results of the sensitivity analysis represent a local optimum in which:

- Small set of the optimization space is tested; not the complete feasible region
- The results are affected by the initial conditions and boundary limits
- The sensitivity analysis in this context allows the user to test the effect of each variable on the objective function, individually.
- However, when all variables are changed simultaneously, their interaction might result in different behavior

Thus, it is important to perform the sensitivity analysis starting from different initial conditions while changing the boundary limits of the optimization variables to assure converging to absolute optimum

The results of the sensitivity analysis of the base case (lean feed at 100 psia) are illustrated in the next section.

3.5.2. Results.

Figure 16 illustrates the behavior of the objective function against the cryogenic compressor outlet pressure (P_{RG2out}). As shown in the graph, when P_{RG2out} increases, the objective function increases up to 115 psia, then further increase in P_{RG2out} causes the objective function to stay constant until about 130 psia. Further increase in P_{RG2out} after 130 psia causes the objective function to decrease. This is due to the increase in the compression power consumption in addition to the substantial increase of the cooling duty in heat exchangers E-103 and E-104 without a major increase in the ethane recovery (SNGL).

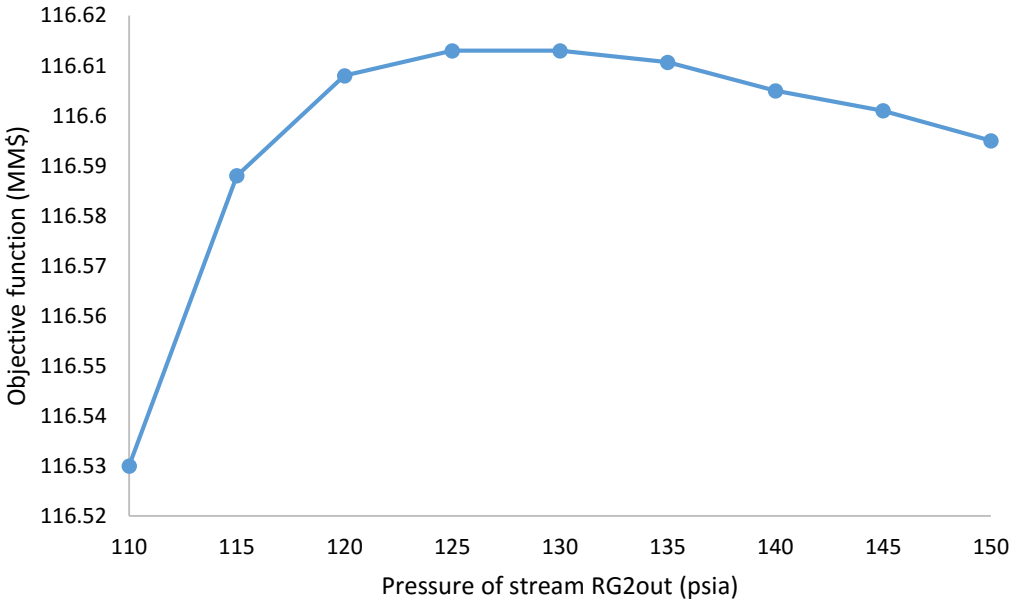

Figure 16: Effect of the cryogenic compressor outlet pressure on the objective function

Figure 17 shows the relationship between the objective function and T_{10}, the temperature of the gas stream leaving the separator after exchanging heat in E-103. When T_{10} decreases (more negative), the objective function slightly oscillates up and down. However, the overall behavior of T_{10} shows that as T_{10} decreases (more negative), the objective function increases. This is because as T_{10} decreases, the temperature profile of the demethanizer is shifted down, hence, increasing ethane recovery and profit, as will be described later in Chapter 4.

Figure 18 shows the behavior of the objective function versus the temperature of the split vapor feed to the demethanizer (T_{12out}). It can be seen that there is no response

in the objective function when T_{12out} increases (less negative) over the small region (-201 to -198°F). The convergence of the simulator is very sensitive to the changes in this variable. Thus, it was not possible to demonstrate the effect of this variable over a wider range.

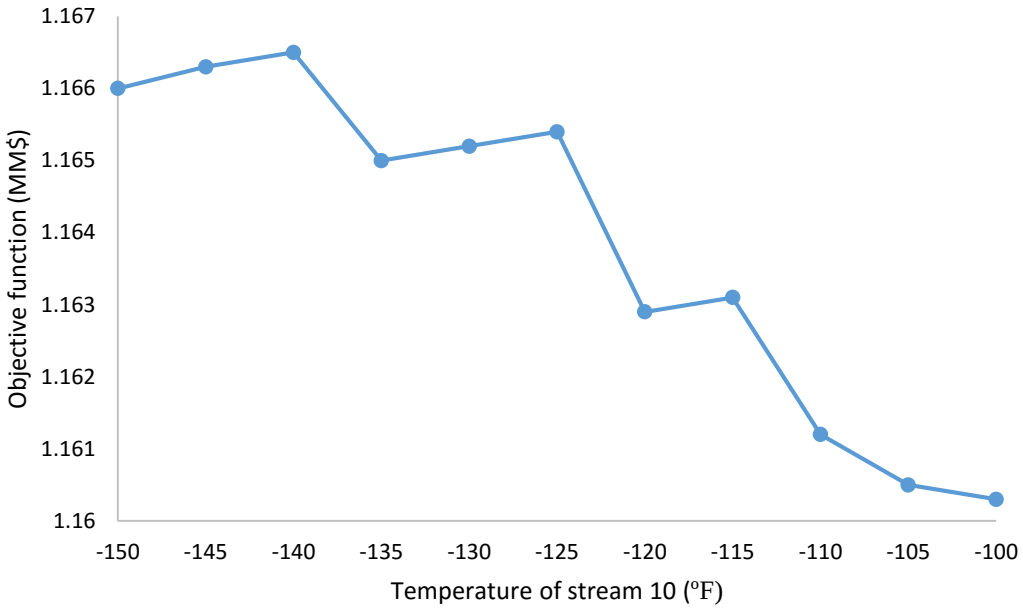

Figure 17: Effect of varying T10 on the objective function

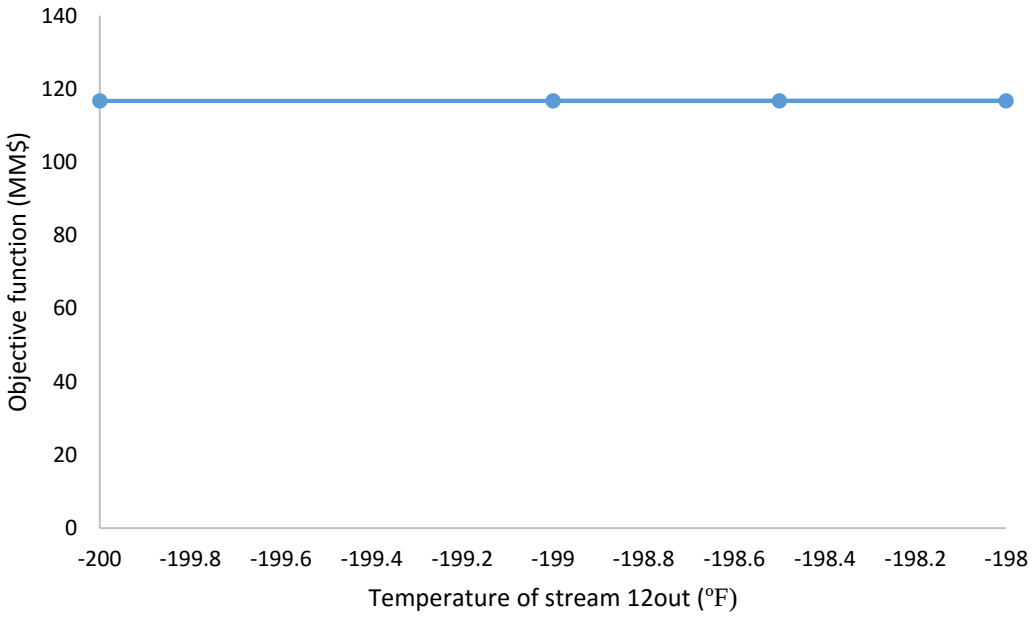

Figure 18: Effect of varying T12 on the objective function

Figure 19 shows the variation of the objective function against the molar flow rate of stream 8 leaving splitter TEE-100. This graph shows that when the molar flow rate of stream 8 was increased from 1000 to 1500 lbmol/hr, the objective function increased substantially. At higher molar flow rates (more than 2000 lbmol/hr), the objective function started to decrease. This might be justified by the fact that less molar flow rate ($\dot{M}_7$) will be sent to the expander which reduces the useful work that can be extracted from the expander. Thus, reducing the sales gas revenue, as more gas will be needed to provide the recompression power.

Figure 20 provides the relationship between the molar flow rate of stream 5out2 in TEE-101 and the objective function. As the molar flow rate of stream 5out2 increases, the objective function experiences a very small change. It can be concluded that the variable does not affect the objective function strongly.

In Figure 21, the variation of the objective function is plotted against the molar flow rate of stream RG2 leaving splitter TEE-102. As the molar flow rate of stream RG2 increases, the objective function decreases. This is due to the fact that any increase in this variable will require additional compression power in the cryogenic compressor (K-100), hence, decreasing the objective function.

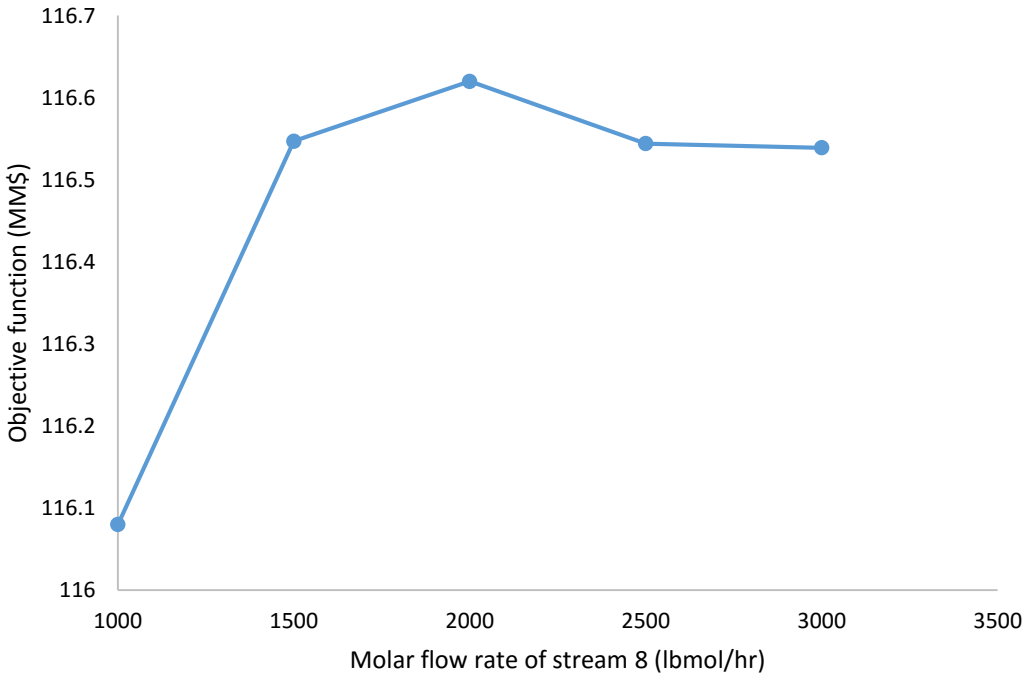

Figure 19: Effect of varying molar flow rate of stream 8 on the objective function

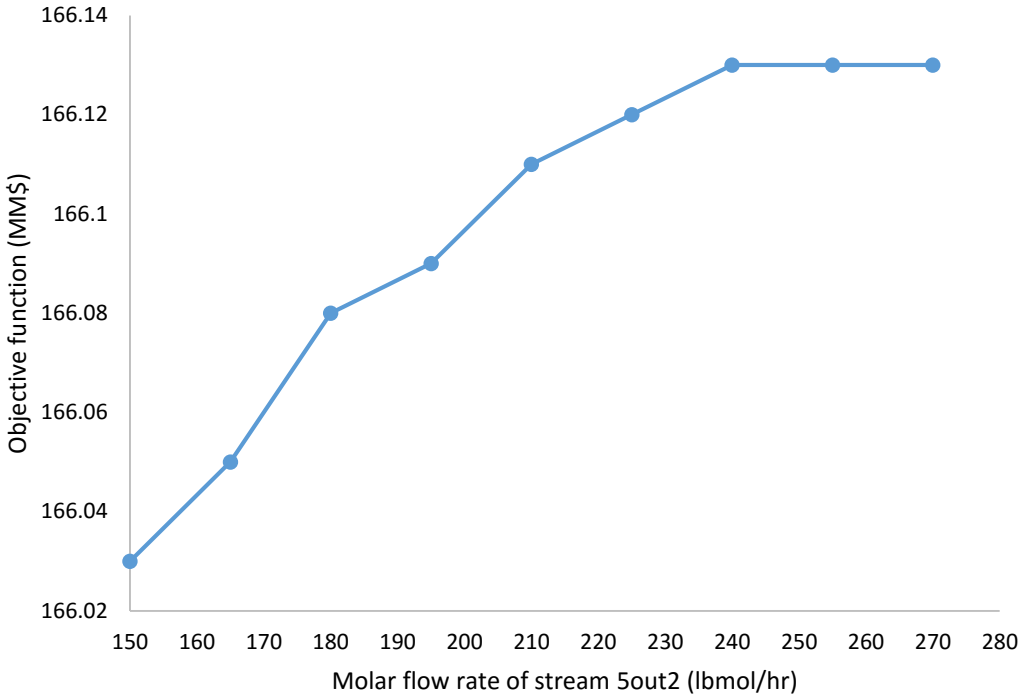

Figure 20: Effect of varying molar flow rate of stream 5out2 on the objective function

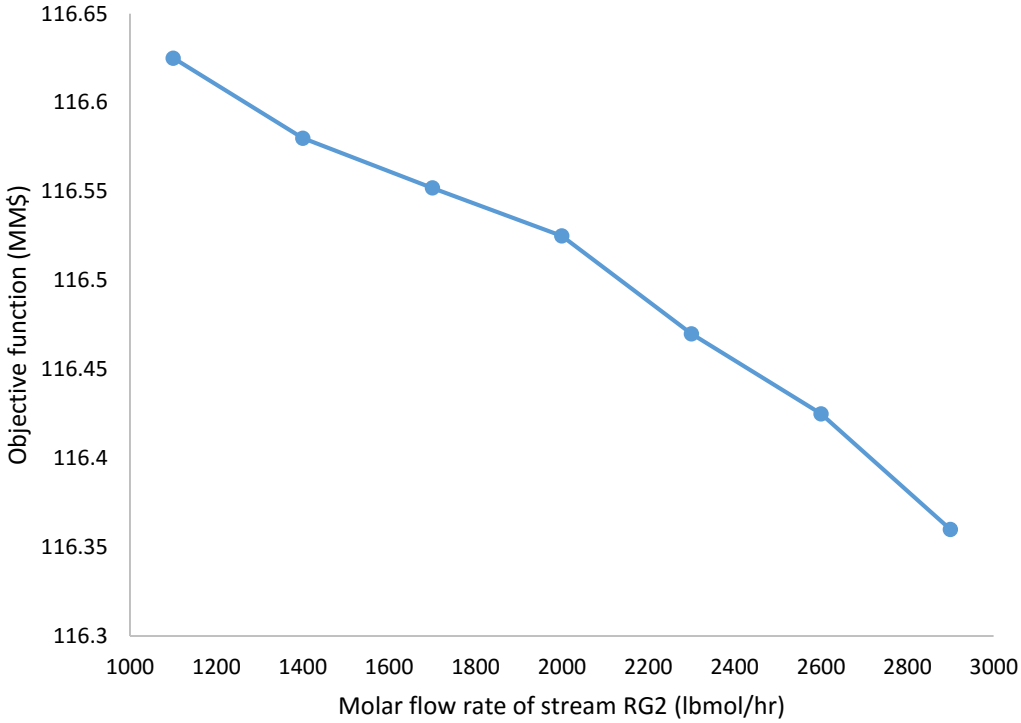

Figure 21: Effect of varying molar flow rate of stream RG2 on the objective function

The results of the sensitivity analysis suggest the following:

1. The key optimization variables are $\dot{M}_8$ and T_{10}. The aforementioned variables had the strongest effect of the objective function
2. Over the simulated region, the objective function favors low P_{RG2out}
3. Over the simulated region, the objective function favors low $\dot{M}_{RG2}$
4. The variable $\dot{M}_{5out2}$ had a very minor effect on the objective function over the simulated region
5. The convergence of the simulator is very sensitive to the variable T_{12out}. Thus, only small variations in this variable are allowed.

Results 2 and 3 suggest that the CRR process may eventually reduce to GSP. This statement is confirmed in the optimization runs as will be illustrated in Chapter 4 afterwards.

3.6. Optimization

This section discusses the optimization algorithm used in addition to the objective function and the optimization variables.

3.6.1. Hyprotech SQP Optimizer.

The optimization work has been conducted using the Hyprotech Sequential Quadratic Programming (SQP) optimizer, a built-in optimizer in HYSYS that was recommended by Aspen Tech. This algorithm has been used to solve more complex problems including many independent variables, constraints, and complex objective function elements. It requires the use of HYSYS Derivative Model Analysis feature to hold all the data. Thus, the first step to set up SQP is to create a Derivative Analysis. The parameters of the optimizer were fixed at their default values as per Aspen's recommendations. The Hyprotech SQP optimizer ensures evaluating the objective function within the variable boundaries [24].

The complexity of the model arises from some of the following points:

1. The complexity of the objective function.
2. The scope of the work is multi-variable optimization.

3. The simulation does not converge when changing the variables. The optimizer runs the simulation hundreds of times to determine the derivatives. If the simulation fails in any stage, then the optimizer will fail. The simulation must be robust to handle the change of variables.

However, it is worth noting that Hyprotech SQP optimizer was able to converge to one objective function for each of the simulated cases without being affected by the different initial guesses that were used. Hyprotech SQP optimizer coped well with the complexity of the flowsheet in comparison with the original optimizer. Additionally, the upper and lower limits of the variables were continuously changed throughout the runs. The aforementioned points can, somehow, assure the convergence of the simulated models at the absolute optimum.

Chapter 4. Results and Discussion

4.1. Optimum Objective Function at Low NGL to Gas Price Ratio

The NGL and natural gas prices for the last eight years were obtained from the U.S. Energy Information Administration. The price of the natural gas was assumed to be 2.97 $/MM BTU, and the NGL price considered was 5.23 $/MM BTU [25]. The capital cost of all equipment was updated based on the chemical engineering plant cost index (CEPCI) for August 2015 [26]. Optimum values of the design variables for all cases are presented in Appedix C.

4.1.1. Comparison between GSP and CRR.

The primary difference between GSP and CRR is that the CRR uses a partially condensed reflux stream comprised mainly of methane with a very small portion of ethane. This stream was fed to the CRR demethanizer to reduce the ethane losses in the vapor stream leaving the demethanizer. The liquid portion of the reflux containing very low amount of ethane and heavier hydrocarbons acts as an absorbing medium that absorbs these components from the raising vapor [9].

On the contrary, ethane losses are higher in the GSP where the demethanizer column is operated as a stripping column. The ethane losses occur as the top feed contains quantities of ethane and heavier hydrocarbons which results in corresponding equilibrium quantities leaving with the vapor stream [9].

The vapor fraction of the reflux stream in the CRR process at all pressures is presented in Table 5. In case of feed A at 100 and 215 psia, the vapor fraction of the recycle stream to the CRR process is around 0.234 and 0.242, respectively. In these cases, most of the methane is in the liquid phase (methane dew point is -205.5 and -175.4 °F, respectively) and the temperature of the recycle stream is -206 and -176.4°F. At 450 psia, the vapor fraction of the recycle stream is 0.963. Most of the methane is in the vapor phase (methane dew point = -139.4°F) and the temperature of the recycle stream is -122.2°F.

If the reflux stream of the optimum CRR process contained a very high vapor fraction, then the reflux stream will not be economically justified and the CRR will be reduced to GSP. The latest case was observed at high demethanizer pressure (450 psia) in case of lean feed as well as all rich feed cases. In case of lean feed, operated at a high

demethanizer pressure, the sales gas leaves the demethanizer at relatively high temperatures that cannot be liquefied easily. In case of the rich feed, most of the liquefiable components leave with the NGL stream at the bottom of the column, whereas the top product consists mainly of the components with the highest vapor pressure.

Table 5: Comparison between the vapor fractions of the recycle stream to the demethanizer at low NGL to gas price ratio

Feed	100 psia	215 psia	450 psia
A	0.234	0.242	0.963
D	0.999	0.999	0.999

The comparison between CRR and GSP in Table 6 was held in the cases where the recycle stream contained adequate quantities of liquid, lean gas at 100 and 215 psia in this case.

In all the aforementioned cases, higher profit was achieved using GSP. Even though the difference in the objective functions is not significant, shows that more complex schemes might not be economically justified. In fact, the CRR reduced to GSP in the cases of lean gas at high demethanizer pressure and all of the rich gas cases. Ethane recovery at 100 psia is higher in the CRR (98.9) compared to GSP (97.8). In the 215 psia case, GSP yielded higher ethane recovery.

Table 6: Comparison between the optimum objective function and the corresponding ethane recovery using CRR and GSP at low NGL to gas price ratio

Process	100 psia		215 psia	
	B (MM$/yr)	Ethane Recovery (%)	B (MM$/yr)	Ethane Recovery (%)
CRR	116.6	98.9	116.4	88.4
GSP	116.7	97.8	116.5	92.0

4.1.2. GSP at different demethanizer pressures.

The objective function was optimized at each demethanizer pressure using the low NGL to gas price ratio. The objective function of feed A was found to decrease with increasing demethanizer pressure (Figure 22). One might predict the objective function of the lean gas evaluated at low price ratio increases with increasing demethanizer pressure because of the higher sales gas profit at high pressures. However, the expenses of external refrigeration surpass the aforementioned effect. No external refrigeration was required for lean feed at low demethanizer pressure which was not the case at higher pressures. Additionally, the optimization results suggest eliminating TEE-101

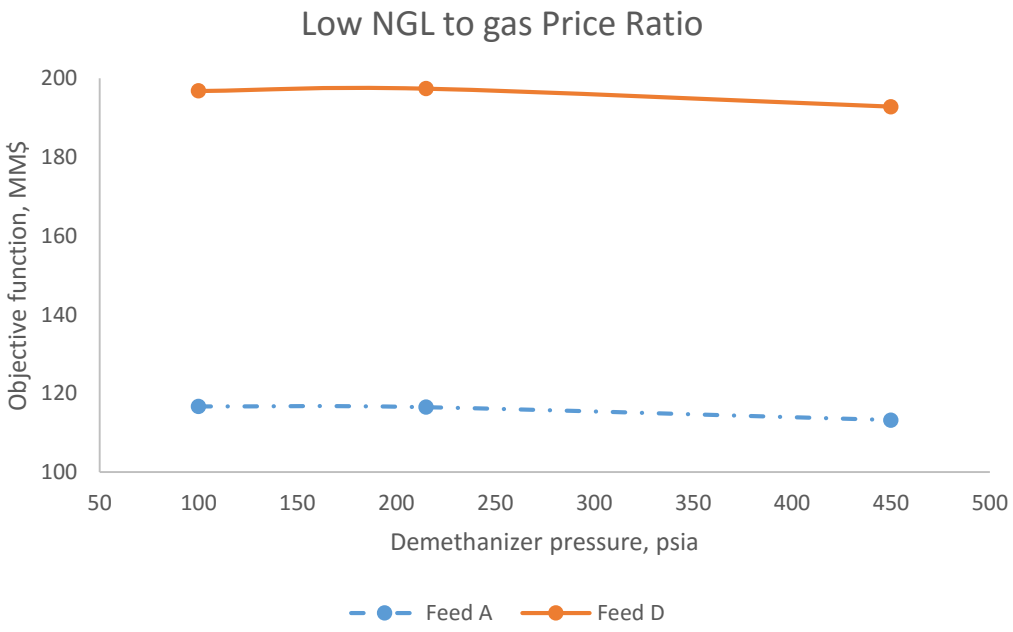

Figure 22: Objective function of feed A at different demethanizer pressures and low NGL to gas price ratios

For feed A, the highest profit was obtained at a demethanizer pressure of 100 psia. At this demethanizer pressure, the utility cost is minimal in comparison to the other pressures for several reasons.

First, no refrigeration is required at 100 psia since self-refrigeration is sufficient to provide the low temperature service at the scrubber (V-100), which is operated at -31°F. This might seem to be somehow contradicting the rule of thumb mentioned in [2, 22, 27]. The rule of thumb states that auto-refrigeration is usually capable of obtaining high ethane recoveries from lean feed gas (less than 2.5 to 3 GPM), while mechanical

refrigeration should be considered in the case of moderately rich feed gas (more than 3 GPM) [2].

The above statement is met in the case of lean gas at low demethanzier pressure, but is violated at intermediate and high demethanzier pressures. This is explained by the fact that at low demethanizer pressure, the temperature of the residue gas is low enough to cool the feed gas which is not the case at higher demethanizer pressures.
The results of feed D (8.6 GPM) confirm the external refrigeration energy requirements stated above.

Second, at the high pressure of 450 psi, steam is used to provide the reboiler heat duty while it is not the case for the other demethanizer pressures of 100 and 215 psi, where the heat duty of the reboiler is provided by the feed.

The profit obtained for feed D is higher than the one obtained for feed A due to the higher NGL content in feed D which is of great significance at high NGL/ gas price ratio. The rich gas curve, on the other hand, shows a peak at a demethanizer pressure of 215 psia. At the intermediate pressure of 215 psia, the highest objective function is reached with a trade-off between the sales gas profit and the NGL profit.

The different costs associated with the objective function are shown in Table 7 and illustrated in the next sections.

4.1.3. Overall capital cost.

In most of the cases, the capital cost of the main process equipment decreases with increasing pressure. The major contributing factor is the capital cost of the compressors. At low demethanizer pressure, the required compressors are larger than the ones required at higher demethanizer rpressures.

4.1.4. Refrigeration cost.

No external refrigeration was required only for the feed A at 100 demethanizer pressure. On the other hand, for feed D, external refrigeration is required for all of the demethanizer pressures. At a demethanizer pressure of 450 psia, the refrigeration cost is the highest. This is due to the fact that at such high pressure, the gas leaving the demethanizer has a lower potential for cooling.

4.1.5. Main process utility cost.

The utility cost of the main process units of feed D is greater than the utility cost of feed A. The utility cost for both feeds associated with mechanical refrigeration is the lowest at a demethanizer pressure of 215 psia. For both feeds, the utility cost associated with mechanical refrigeration is the lowest at a demethanizer pressure of 215 psia.

Table 7: Optimization results of low NGL/gas price ratio

Feed	P (psia)	C_{UT} (MM$/yr)		FCI (MM$)		Total FCI (MM$)	Objective function (MM$/yr)	Ethane recovery (%)
		Main process	Refrigeration cycle	Main process	Refrigeration cycle			
A	100	0.0123	-	21.877	-	21.877	116.7	97.8
	215	-	0.30	16.107	6.7413	22.848	116.5	92
	450	0.113	0.57	9.7798	10.001	19.780	113.2	32.5
D	100	0.015	0.92	17.134	15.517	32.651	196.8	91.2
	215	-	0.77	18.868	13.1688	32.037	197.4	85
	450	0.583	1.20	9.894	19.222	29.116	192.8	72.1

4.2. Optimum Objective Function at High NGL to Gas Price Ratio

The NGL and natural gas prices for the last eight years were obtained from the U.S. Energy Information Administration. The highest NGL to gas price ratio was 3.99 ($/MMBTU)/ ($/MMBTU) [25]. The optimization of the high price ratio was performed based on this value. The price of the natural gas was assumed to be 2.97 $/MM BTU [25]. The NGL price was calculated based on the above two values and found to be 11.13 $/MM BTU. The capital cost of all equipment was updated based on the chemical engineering plant cost index (CEPCI) for August 2015 [26]. Optimum values of the design variables for all cases are presented in Appedix C.

4.2.1. Comparison between GSP and CRR.

The conclusions stated in the previous section also apply to the CRR cases evaluated at high NGL/gas price ratio as illustrated in Table 8 and Table 9.

Again, higher profit is achieved using GSP for all cases except for lean gas at 100 psia. In that case, the ethane recovery and the objective function for the CRR process are higher compared to GSP. CRR at 215 psia gives a lower ethane recovery than GSP.

Table 8: Comparison between the vapor fractions of the recycle stream to the demethanizer at high NGL to gas price ratio

Feed	100 psia	215 psia	450 psia
A	0.08	0.099	0.947
D	0.999	0.999	0.999

Table 9: Comparison between the optimum objective function and the corresponding ethane recovery using CRR and GSP at high NGL to gas price ratio

Process	100 psia		215 psia	
	B (MM$/yr)	Ethane Recovery (%)	B (MM$/yr)	Ethane Recovery (%)
CRR	148.0	98.7	146.5	88.1
GSP	147.9	97.8	147.0	92.0

4.2.2. CRR/GSP at different demethanizer pressures.

Similar to Section 4.1, the analysis is repeated here in the case of high NGL to gas price ratio. As shown in Figure 23, the objective function of the lean gas has an optimum at a demethanizer pressure of 215 psia. One might predict the objective function of the lean gas evaluated at high price ratio to decrease with increasing demethanizer pressure because of the lower NGL content recovered at high demethanizer pressures. However, the expenses of recompressing the sales gas at low demethanizer pressures might have surpassed the aforementioned effect. The recompression cost is the maximum at low demethanizer pressure.

The profit obtained by feed D is higher than the one obtained for feed A due to the higher NGL content in feed D. The objective function obtained using feed D decreases with increasing demethanizer pressure because more NGL is recovered at lower demethanizer pressure in which lower temperature profile is recorded, which

leads to more condensation. The additional NGL recovered compensates for further recompression costs at low demethanizer pressures. This is not the case at the low price ratio discussed earlier.

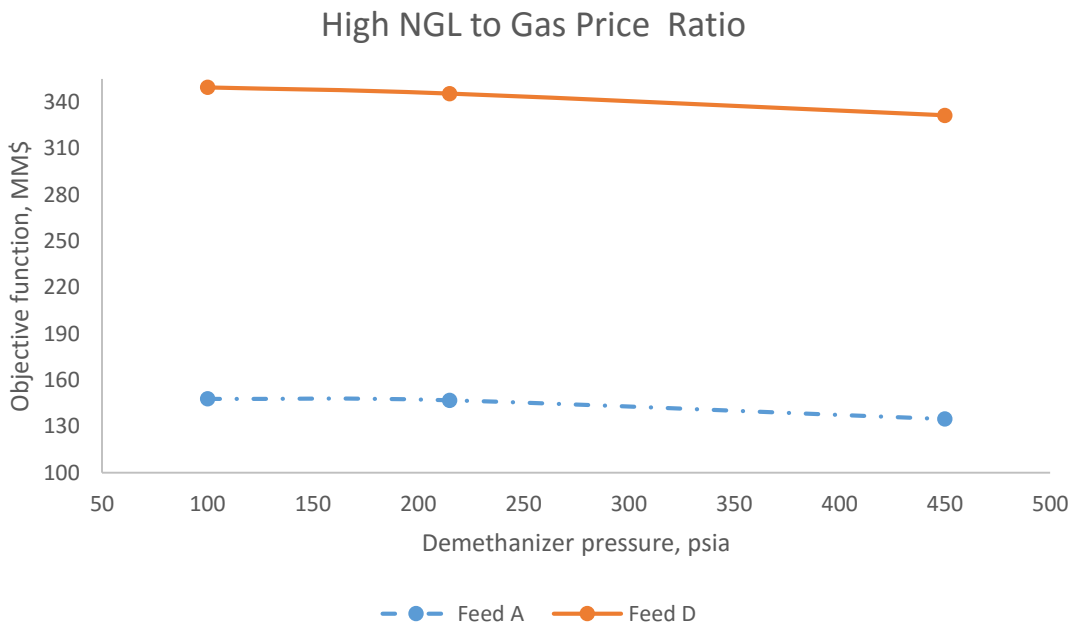

Figure 23: Objective function of feed D at different demethanizer pressures and high NGL to gas price ratios

The results of the optimization at high price ratio are illustrated in Table 10 As in the case of the low price ratio where feed D is used, the refrigeration costs (utilities and fixed capital investment) were the minimum for the 215 psia pressure. Moreover, the refrigeration cost increases with increasing pressure. The capital cost of the main process units decreases with increasing demethanizer pressure.

Table 10: Optimization results of high NGL to gas price ratio

Feed	P (psia)	C_{UT} (MM$/yr)		FCI (MM$)		Total FCI (MM$)	Objective function (MM$/yr)	Ethane recovery (%)
		Main process	Refrigeration cycle	Main process	Refrigeration cycle			
A	100	0.012	-	21.88	-	21.88	147.9	97.8
	215	-	0.30	16.11	6.91	23.02	147.0	92
	450	0.107	0.50	9.52	8.49	18.01	134.5	29.05
D	100	0.011	0.91	21.11	15.69	36.80	349.6	91.2
	215	-	0.78	18.87	13.61	32.49	345.6	85
	450	0.583	1.2	9.21	18.76	27.97	331.5	72.1

4.2.3. Comparison of the current work with published work.

The optimization results of the GSP process are in good agreement with the results reported by Kherbeck and Chebbi [12]. In fact, maximizing the profit-related objective function resulted in the maximum ethane recoveries reported in [12].

Figure 24 illustrates the comparison between the ethane recoveries as obtained by CRR/GSP and conventional turboexpander processes at low and high NGL to Gas price ratios. The data of the results of the turboexpander process was found in [4]. In all cases, the ethane recovery of the CRR/GSP were found superior to the conventional turboexpander process except for the high/low NGL to gas price ratio cases of lean feed at 450 psia demethanizer pressure.

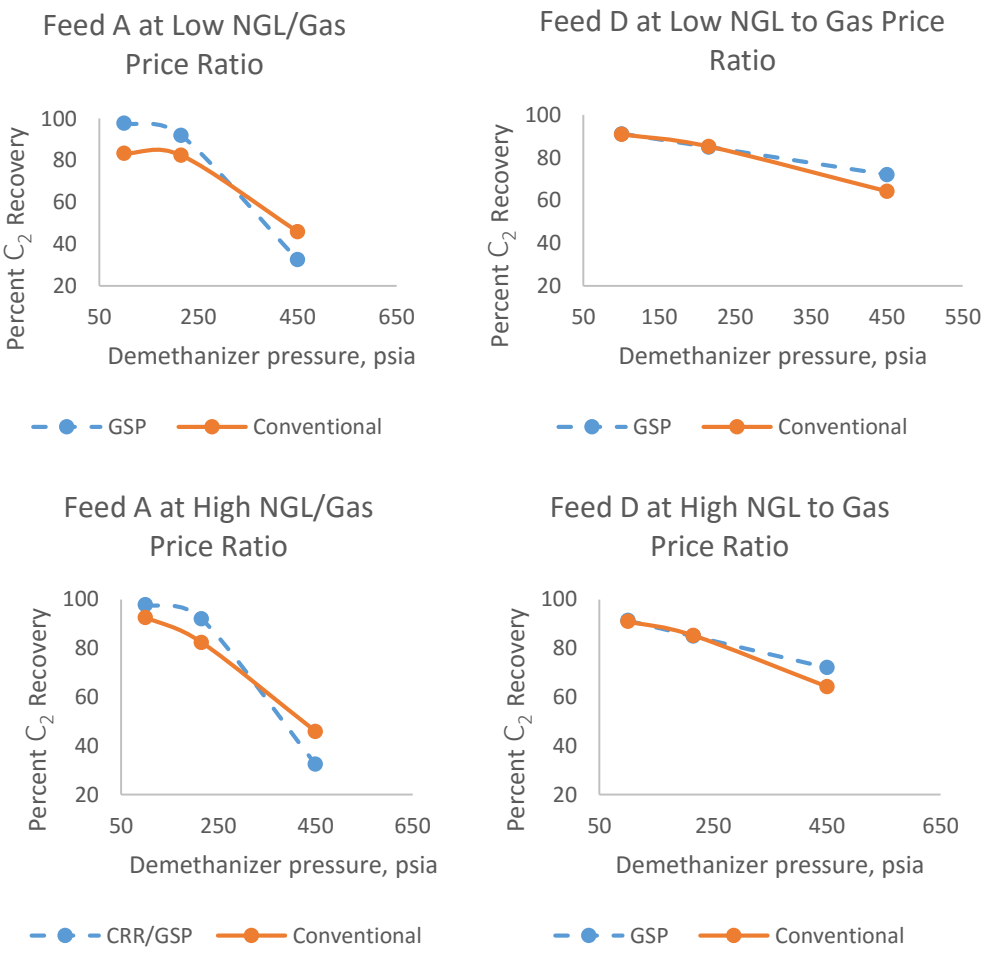

Figure 24: Ethane recoveries as obtained using optimum objective functions in the GSP and conventional turboexpander processes

In the current work, high ethane recoveries were achieved using leaner feed to the process while operating the demethanizer column at the same pressure. This might mean that a leaner feed to the process results in a leaner recycle feed to the demethanizer that is capable of absorbing the relatively heavier hydrocarbon components.

Having said that, the inventors of the CRR emphasized the point that the composition of the recycle stream to the demethanizer dedicates the ultimate ethane recovery. Another important point was also stated in the patent [9]: in order to achieve high ethane recoveries at the same demethanizer pressure, a leaner recycle should be used.

The effect of demethanizer pressure on ethane recovery was well illustrated in CRR inventory [9] where it was stated that the demethanizer should be operated at low pressures in order to achieve high ethane recoveries. This will increase the ethane recovery on one hand, but will increase the compression costs, on the other hand.

4.3. CO_2 Frost Point

CO_2 frost is one of the key factors that contributes to the process selection. Some processes are CO_2 tolerant-that is they are capable of achieving almost the same ethane recoveries without crossing the CO_2 frost point. If the NGL recovery process is CO_2 tolerant, the cost of removing CO_2 may be reduced [20].

The different processes can be compared for CO_2 tolerance by calculating the CO_2 frost temperature approach (ΔTCO_2) [28]. The lowest CO_2 frost temperature approach is calculated using the lowest demethanizer feed temperature and the predicted CO_2 frost temperature for that stream. If the value of the CO_2 frost temperature approach is negative, this suggests that a CO_2 freezing problem will most likely occur [28].

$$\Delta T_{CO_2} = T_{\text{Coldest Feed}} - T_{CO_2\ \text{Frost}} \quad [28]$$

4.3.1. CO_2 tolerance in GSP and CRR processes.

In this section, the effect of CO_2 is studied using the optimum GSP at all demethanizer pressures and CRR at 100 psia. In order to input a composition that would be accepted by HYSYS, the percentage of methane was reduced and replaced by CO_2 until the CO_2 frost point composition was reached. All of the CO_2 related simulations were carried at low NGL to gas price ratio.

Table 11: CO_2 tolerance in GSP and CRR processes at low NGL to gas price ratio

Process	CO_2 content (%)	Lowest temperature in the column (°F)	CO_2 frost point (°F)	ΔT_{CO_2}	B (MM$/yr)	Recovery (%)
GSP	0.4	-203.3	-205.2	1.9	116.4	97.6
CRR	0.4	-206	-210.7	4.7	116.1	98%

The 100 psia with CO_2 case was simulated using GSP and CRR. The results indicate slightly higher profit for the GSP whereas the CRR yields higher ethane recovery. For the same CO_2 content (0.4%), the frost temperature approach of the CRR is higher than that of GSP for comparable ethane recoveries (% difference is 0.4). Thus, CRR process is more CO_2-tolerant than GSP.

4.3.2. CO_2 tolerance for lean feed at different demethanizer pressures.

As stated earlier in Chapter 4 , the CRR is economically justified only when enough liquid is recycled to the top of the column. Otherwise, the GSP is superior.

Table 12: CO_2 analysis for lean feed at low NGL to gas price ratio

Pressure (psia)	CO_2 content (%)	Lowest temperature in the column (°F)	CO_2 frost point (°F)	ΔT_{CO_2}	B (MM$/yr)	Recovery (%)
100	0.4	-203.3	-205.2	1.9	116.4	97.6
215	1	-167	-172.5	5.5	115.4	89.5
450	2	-103	-136.1	33.1	111.4	35.7

With regard to the 100 and 215 psia cases without CO_2 (Table 7), adding CO_2 to the feed decreased both profit and the recovery as compared to the cases with zero-CO_2 (Table 12). When recovering ethane at low and intermediate demethanizer pressures, the demethanizer column overhead is operated at very low temperatures between -170 and -210 °F according to the demethanizer pressure. Such operating temperatures are well below the frost point of a pure CO_2 stream (-109 °F). These temperatures might not be achievable because of the CO_2 frost point, hence, lowering both of ethane recovery and profit. At high demethanizer pressures, on the other hand, the temperature profile of the column is shifted up, hence, reducing the possibility of solid CO_2 formation and lowering ethane recovery as well.

The simulation of the 450 psia using a lean feed containing CO_2 yielded a lower profit, but a higher ethane recovery. The vapor pressure of CO_2 is intermediate between

methane and ethane [22]. Thus, the CO_2 replaces most of the ethane in the overhead product and ethane will be mostly available in the NGL stream (higher ethane recovery). Moreover, the methane to ethane ratio is set at 0.02 in all cases. Thus, due to high ethane recovery, and in order to keep the ratio between methane and ethane fixed in the NGL stream, more methane is recovered at the bottoms of the demethanizer. Thus, the sales gas revenue will be reduced compared to the case with zero-CO_2. Apparently, the aforementioned reason affected the demethanizer operated at 450 psia more than the other cases.

4.3.3. CO_2 tolerance for rich feed at different demethanizer pressures.

In all of the GSP cases (Table 12 and Table 13), the CO_2 frost temperature approach increases with the demethanizer pressure. Further, the CO_2 content either increased (all of lean gas cases as well as rich gas at 100 and 215 psia) or remained the same (rich feed at 215 and 450 psia). The previously mentioned points can be explained by the fact that operating the demethanzier at high pressures raises the temperature profile in the column. The CO_2 recovery decreased at higher demethanizer pressures following the same trend observed previously.

Table 13: CO_2 analysis for rich feed at low NGL to gas price ratio

Pressure (psia)	CO_2 content (%)	Lowest temperature in the column (°F)	CO_2 frost point (°F)	ΔT_{CO_2}	B (MM$/yr)	Recovery (%)
100	1	-166.1	-173	6.9	196.6	90
215	2	-132	-151.1	19.1	195.5	84.6
450	2	-82.5	-144.2	61.7	190.8	72.3

Tables 11 and 12 show that the CO_2 frost temperature approach is higher in rich feed cases in comparison to the lean feed cases. This can be justified by the fact that the lean gas processing involves much lower demethanizer temperatures than the rich gas.

Chapter 5. Conclusion

The Cold Residue Recycle (CRR) process and the Gas Subcooled Process (GSP) were optimized at three demethanizer pressures; 100, 215 and 450 psia. Moreover, the analysis was conducted at two different feed compositions. The optimization objective function was evaluated either using high or low NGL to gas price ratios. In the current work, the effects of several design variables on the profit-related objective function were analyzed. The optimization of the Cold Residue Recycle (CRR) process and the Gas Subcooled Process (GSP) revealed that in most cases, the GSP yields a higher profit except for the lean gas evaluated at low demethanizer pressure and high NGL to gas price ratio. In this particular case, the CRR yields a relatively higher profit and higher ethane recovery. External refrigeration is required for optimization in all cases except for the case of lean feed gas operated at 100 psia demethanizer pressure. The optimum results suggest eliminating one splitter in the case of lean feed at 100, 215 and 450 psia demethanizer pressures. As far as CO_2 tolerance is concerned, GSP was compared to CRR process at 100 psia demethanizer pressure. The findings show that CRR is more CO_2 tolerant than GSP.

References

[1] U.S. Energy Information Administration (EIA). “What are natural gas liquids and how are they used?”" [Online]. Available: http://www.eia.gov/todayinenergy/detail.cfm?id=5930. April, 20, 2012 [Nov. 5, 2014].

[2] F. S. Manning and R. E. Thompson. *Oil Field Processing of Petroleum*, Tulsa: PennWell Publishing Company, 1991.

[3] A. Chamberlin. “What is ethane and is it important for energy companies?” [Online]. Available: http://marketrealist.com/2014/04/ethane-important-energy-companies/. April, 11, 2014 [Dec. 30, 2014].

[4] R. Chebbi, N. S. Al-Amoodi, N. M. Abdel Jabbar, G. A. Husseini and K. A. Al-Mazroui. "Optimum ethane recovery in conventional turboexpander processes," *Chemical Engineering Research and Design,* vol. 88, no. 5-6, pp. 779-787, 2010.

[5] D. MacKenzie and S. Donnelly. "Mixed refrigerant proven efficient in natural gas liquids recovery process," *Oil and Gas,* vol. 83, no. 9, pp. 116-120, 1985.

[6] R. McKee. "Evolution in Design," in *56th Annual GPA convention*, 1977.

[7] R. Lee, J. Yao and D. Elliot. "Flexibility, efficiency to characterize gas-processing technologies," *Oil and Gas,* vol. 97, no. 50, pp. 90-94, 1999.

[8] R. Chebbi, A. Al-Qaydi, A. Al-Amery, N. Al-Zaabi and H. Al-Mansouri. "Simulation study compares ethane recovery in turboexpander processes," *Oil and Gas,* vol. 102, no. 4, pp. 64-67, 2004.

[9] R. Campbell, J. Wilkinson and H. Hudson. "Hydrocarbon gas processing". U.S. Patent 05,568,737, October, 29, 1996.

[10] "Hydrocarbon Recovery," in *GPSA Engineering Data Book*, Tulsa, Gas Processors Suppliers Association, 2004.

[11] M. Diaz, A. Serrani, J. Bandoni and E. Brignole. "Automatic Design and Optimization of Natural gas Plants," *Industrial and Engineering Chemical Research*, vol. 36, no. 7, pp. 2715-2724, 1997.

[12] L. Kherbeck and R. Chebbi. "Optimizing ethane recovery in turboexpander processes," *Industrial and Engineering Chemical Research,* vol. 21, pp. 292-297, Mar. 2014.

[13] R. E. Campbell, J. D. Wilkinson and H. M. Hudson. "Hydrocarbon gas processing". U.S. Patent 04,889,545 A, December, 1, 1989.

[14] R. Chebbi, K. A. Mazroui and N. M. AbdelJabbar. "Study compares C_{2+} recovery for conventional turboexpander, GSP," *Oil and Gas,* vol. 106, no. 46, pp. 50-54, 2008.

[15] K. Jibril, A. Humaizi, A. Idriss and A. Ibrahim. "Simulation study determines optimum turboexpander process for NGL recovery," *Oil and Gas,* vol. 104, no. 9, pp. 58-62, 2006.

[16] R. Lee, Y. Zhang, J. Yao and J. Juh Che. "Internal refrigeration for enhanced NGL recovery". U.S. Patent 07,257,966, August, 21, 2007.

[17] M. Getu, S. Mahadzirb, N. Van Duc Longc and M. Lee. "Techno-economic analysis of potential natural gas liquid (NGL) recovery processes under variations of feed compositions," *Chemical Engineering Research and Design*, vol. 91, no. 7, pp. 1272-1283, 2013.

[18] M. Mehrpooya, F. Gharagheizi and A. Vatani. "An optimization of capital and operating alternatives in a NGL recovery unit," *Chemical Engineering and Technology,* vol. 29, no. 12, pp. 1469-1480, 2006.

[19] M. Mehrpooya, F. Gharagheizi and A. Vtani. "Introducing a new parameter for evaluating the degree of integration in cryogenic liquid recovery processes," *Chemical Engineering and Processing: Process Intensification,* vol. 50, no. 9 , pp. 916-930, 2011.

[20] S. Mokhatab, W. A. Poe, J. G. Speight and I. Ebrary. *Handbook of Natural Gas Transmission and Processing*, Burlington: Gulf Professional Pub., 2006.

[21] G. L. Kaes. "A practical guide to steady state modeling of petroleum processes (using commercial simulators)," Athens Printing Company, 2000.

[22] A. J. Kidnay, W. R. Parrish and D. G. McCartney. *Fundamentals of natural gas processing* (2nd ed.), Boca Raton: FL: CRC Press, 2011.

[23] R. Turton, R. C. Bailie, W. B. Whiting and J. A. Shaeiwitz. *Analysis, synthesis, and design of chemical processes* (4th ed.), Upper Saddle River: NJ: Prentice Hall., 2012.

[24] "Aspen HYSYS petroleum refining (V7.3), Unit Operations Guide," Aspen Technology, Inc, Burlington, 2011.

[25] U.S. Energy Information Administration (EIA). “U.S. Natural Gas Liquid composite price” [Online]. Available: http://www.eia.gov/dnav/ng/hist/ngm_epg0_plc_nus_dmmbtum.htm. [May, 15, 2014].

[26] S. Jenkins. *Current Economic Trends: November 2015* [Online]. Available: http://www.chemengonline.com/current-economic-trends-november-2015/. Jan. , 19, 2015 [Nov., 5, 2015].

[27] D. N. Ewan, J. B. Lawrence, C. L. Rambo and R. R. Tonne. "Why cryogenic processing (Investigating the Feasibility of Cryogenic Turbo-Expander Plant," in *54th GPA Annual Convention*, Houston, 1975.

[28] K. A. Pennybaker, S. W. Wolerton, S. W. Chafin, T. R. Ruddy and C. W. Pritchard. "A comparative study of ethane recovery processes," in *79th GPA Annual Convention*, Atlanta, Georgia, 2000.

[29] P. Wankat. *Separation Process Engineering: Includes mass transfer catalysis* (3rd ed.), Upper Saddle River, NJ: Prentice Hall, 2012.

[30] J. M. Douglas. *Conceptual Design in Chemical Processes*, Boston: McGraw-Hill, 1988.

[31] R. K. Sinnott, J. M. Coulson, J. F. Richardson and I. Ebrary. *Chemical Engineering Design* (4th ed.), Oxford: Elsevier Butterworth-Heinemann, 2005.

[32] A. Biegler, L. Grossman and I. Westerberg. *Systematic Methods of Chemical Process Design*, New Jersey: Prentice Hall, 1997.

[33] A. McDonald and H. Magande. "Heat Exchanger Design," in *Introduction to Thermofluids Systems Design* (1st ed.), J. Wiley and Sons, 2012.

Appendix A: Equipment sizing

Appendix A provides the equations used in sizing the different unit operations in the CRR process based on heuristics in chemical engineering. This includes sizing of the demethanizer, heat exchangers, compressors and vessels.

A1. Demethanizer

Equation A1.1 [29] can be used to evaluate the flooding velocity for the design of the demethanizer

$$U_F = C_{sb} \times \sqrt{\frac{\rho_L - \rho_V}{\rho_V}} \times \left(\frac{\sigma_{top}}{20}\right)^{0.2} \quad \text{(A1.1)}$$

where U_F= flooding velocity, ft/sec

ρ_L= liquid density, Ib/ft^3

ρ_V = vapor density, Ib/ft^3

σ_{top} = surface tension, dyne/ cm

C_{sb} = capacity factor at tray spacing of 24" is found using

$$\log_{10} C_{sb} = -0.94506 - 0.70234 \log_{10} F_{lv} - 0.22618 (\log_{10} F_{lv})^2 \quad \text{(A1.2)}$$

where F_{lv} is calculated using

$$F_{lv} = \frac{W_L}{W_V}\sqrt{\frac{\rho_V}{\rho_L}} \quad \text{(A1.3)}$$

Equation A1.2 [29] is used to evaluate the cross sectional area of the demethanizer

$$A = \frac{\overline{V}}{0.9 \times \rho_V \times 0.6 \times U_F} \quad \text{(A1.4)}$$

where A= cross sectional area of the demethanizer, ft^2

$\overline{V}$= molar flow rate of the vapor leaving the top of the column, $lbmole/sec$

The diameter of the demethanizer is given by equation A1.3

$$D_C = \sqrt{\frac{4\,A}{\pi}} \quad \text{(A1.5)}$$

where D_C = diameter of the demethanizer, ft

The height of the column is given by

$$H_C = TS * AV * N_{actual} \quad \text{(A1.6)}$$

where H_C = height of the demethanizer, ft

TS= tray spacing

N_{actual} = actual number of trays

AV= allowance for vapor disengagement at the ends of the column, it is considered to be 15% of the original height [30]

In order to get the actual number of trays, equation (A1.5) [23] is used

$$N_{actual} = \frac{N_{theoretical}}{E_o} \quad \text{(A1.7)}$$

where $N_{theoretical}$ = theoretical number of trays

E_o = overall tray efficiency. Value was taken as 0.45 based on [21]

A2. Heat exchangers

The general equation [23] used to evaluate the area of the heat exchanger is

$$A_{HE} = \frac{Q}{F * U_o * \Delta T_{lm}} \quad \text{(A2.1)}$$

where A_{HE}= heat exchanger area, ft^2

Q= duty of the heat exchanger, $\frac{Btu}{hr}$

F= correction factor

U_o = overall heat transfer coefficient for cooling/ heating fluid[1], $\frac{Btu}{hr.°F.ft^2}$

ΔT_{lm}= logarithmic mean temperature difference given by equation A2.2 [23]

$$\Delta T_{lm} = \frac{(T_{h,i} - T_{c,o}) - (T_{h,o} - T_{c,i})}{\ln\left(\frac{T_{h,i} - T_{c,o}}{T_{h,o} - T_{c,i}}\right)} \quad \text{(A2.2)}$$

where $T_{h,i}$= inlet temperature of the hot stream, °F

$T_{c,o}$= outlet temperature of the cold stream, °F

$T_{h,o}$= outlet temperature of the hot stream, °F

[1] The value for U_o used for heat exhangers is 64 $\frac{Btu}{hr.°F.ft^2}$ [32]. For air coolers, $U_o is$ 45 $\frac{Btu}{hr.°F.ft^2}$ [33]

$T_{c,i}$= inlet temperature of the cold stream, °F

A3. Compressors

The fluid power for a compressor is calculated by the following equation [23]

$$\dot{W}_f = \frac{m * z_1 * R * T_1 * \left[\left(\frac{P_2}{P_1}\right)^a - 1\right]}{a} \quad \text{(A3.1)}$$

where $\dot{W}_f$= fluid power, Btu/sec

$\dot{m}$= molar flow rate of the inlet gas, $lbmole/sec$

T_1= temperature of the inlet stream to the compressor, R

P_1 = pressure of the inlet stream to the compressor, psia

Z_1 = Compressibility factor of the inlet stream to the compressor

P_2 = pressure of the outlet stream of the compressor, psia

R = real gas constant is

$a = \frac{k-1}{k}$ and $k = \frac{C_P}{C_v}$

The shaft power is given by:

$$\dot{W}_s = \frac{\dot{W}_f}{\varepsilon_{sh}} \quad \text{(A3.2)}$$

where $\dot{W}_s$= shaft power, Btu/sec

ε_{sh}= shaft efficiency, assumed to be 75%

The drive power is calculated by equation A3.5 [23]

$$\dot{W}_d = \frac{\dot{W}_s}{\varepsilon_{drive}} \quad \text{(A3.3)}$$

where $\dot{W}_d$= drive power, Btu/sec

ε_{drive}= drive efficiency

Equation A3.4 [23] in case of gas engine/ gas turbine drive gives

$$\varepsilon_{\text{gas engine}}(\%) = 10 + 11\log_{10}(W_s) - [\log_{10}(W_s)]^2 \quad \text{(A3.4)}$$

where $\varepsilon_{\text{gas engine}}$ = efficiency of the gas engine/gas

If two-stage compressors are required, the intermediate pressure as

$$P_i = \sqrt{P_1\, P_2} \quad \text{(A3.5)}$$

where P_i = intermediate pressure, psia

P_1= pressure at the inlet to the first compressor, psia

P_2= pressure at the outlet of the second compressor, psia

A4. Flash drum

The permissible vapor velocity of a vertical vessel with a demister is calculated by [31]

$$u_{perm} = K_{drum} \sqrt{\frac{\rho_L - \rho_V}{\rho_V}} \quad \text{(A4.1)}$$

where u_{perm}= permissible velocity, ft/sec

ρ_L= liquid density, Ib/ft^3

ρ_V= vapor density, Ib/ft^3

K_{drum}= 0.23 ft/sec [31]

The cross sectional area of the vessel is calculated by [29]

$$A_c = \frac{V * MW_V}{u_{perm} * \rho_V} \quad \text{(A4.3)}$$

where A_c= cross sectional area, ft^2

V= vapor flow rate, Ib/sec

MW_V=molecular weight of the vapor stream, $lb/lbmole$

The diameter of the vessel is given by

$$D_V = \sqrt{\frac{4\,A_c}{\pi}} \quad \text{(A4.4)}$$

where D_V = diameter of the vessel, ft

Appendix B: Costing

To evaluate the objective function (Eq.9), the sales gas, sales of natural gas liquid and the fixed capital investment are needed. All details are provided below.

$$\mathrm{SG} = \mathrm{NG\ price} \times \mathrm{HHV} \times \dot{m} \tag{B.1}$$

where SG = sales of natural gas, $\$/\mathrm{yr}$

NG price =natural gas price, $\frac{\$}{\mathrm{MMBTU}}$

HHV= higher heating value of the sales gas, $\mathrm{Btu/lbmole}$

$\dot{m}$ = molar flow rate of sales gas, $\mathrm{lbmole/yr}$

The sales of the natural gas liquid is given by

$$\mathrm{SNGL} = \mathrm{NGL\ price} \times \mathrm{HHV} \times \dot{m} \tag{B.2}$$

where SNGL = sales of natural gas liquid, $\$/\mathrm{yr}$

NGL price =natural gas Liquids price, $\frac{\$}{\mathrm{MMBTU}}$

HHV= higher heating value of the natural gas liquids, $\mathrm{Btu/lbmole}$

$\dot{n}$= molar flow rate of NGL, $\mathrm{lbmole/yr}$

The bare module cost for the equipment can be calculated by [23]

$$C_{BM} = C_P^{\circ} F_{BM} = C_P^{\circ} (B_1 + B_2 F_M F_P) \tag{B.3}$$

where C_P° = purchased cost of the equipment, given by [23]

$$\log_{10} C_P^{\circ} = K_1 + K_2 \log_{10}(A) + K_3 [\log_{10}(A)]^2 \tag{B.4}$$

where A = size attribute for each equipment

K_1, K_2, K_3= constants given in Table 4 [23]

F_{BM} = bare module factor that is found directly for certain equipment. Alternatively, pressure factor (F_P) can be evaluated using equation B.5 (for all process equipment except process vessels) or B.6 (for process vessels) along with constants B_1, B_2 and material factor (F_M) obtained from Table 4 [23] and presented in Table 14.

$$\log_{10} F_p = C_1 + C_2 \log_{10} P + C_3 (\log_{10} P)^2 \quad \text{(B.5)}$$

$$F_{p,vessel} = \frac{\frac{(P+1)D_V}{2[850 - 0.6(P+1)]} + CA}{t_{min}} \quad \text{for } t > t_{min}, p > -0.5 \text{ barg} \quad \text{(B.6)}$$

where P = pressure, barg

C_1, C_2, C_3 = constants available in Table 4

CA= corrosion allowance, assumed to be 0.00315 m

t_{min}= minimum allowable thickness of a vessel, assumed to be 0.0063 m

$F_{p,vessel}$= pressure factors for vessels

D_V = diameter of the vessel, ft

The utility cost is calculated using equation B.7

$$C_{utility} = \sum C_{BM_u} \quad \text{(B.7)}$$

where $C_{utility}$ = utility cost, \$/yr

C_{BM_u}= bare module cost of the utilities, \$/yr

Table 14: Cost data, pressure factor and material factor of the main process units [23]

Equipment	Type	Material	C_1	C_2	C_3	F_P	B_1	B_2	F_M	F_{BM}	K_1	K_2	K_3
Demethanizer	Distillation Column	SS	-	-	-	2.804	2.25	1.82	3.1	18.07	3.4974	0.4485	0.1074
Trays	Sieve trays	SS	-	-	-	1.0	-	-	-	1.8	2.9949	0.4465	0.3961
Reboiler	Thermosyp-hon vertical	CS shell CS tube	0.1578	0.2992	0.1413	1.332	-	-	-	5.10	4.642	0.3698	2.50e-3
E-100	U-tube	CS shell CS tube	3.88e-2	-0.11272	8.18e-2	1.382	1.63	1.66	1.0	3.924	4.1884	-0.2503	0.1974
E-101	U-tube	CS shell CS tube	3.88e-2	-0.1127	8.18e-2	1.382	1.63	1.66	1.0	3.924	4.1884	-0.2503	0.1974
E-102	U-tube	CS shell SS tubes	3.88e-2	-0.1127	8.18e-2	1.382	1.63	1.66	1.8	5.53	4.1884	-0.2503	0.1974
E-103	U-tube	SS shell SS tube	0	0	0	1.0	1.74	1.55	2.73	5.925	3.9912	6.68e-2	0.243
E-104	U-tube	SS shell SS tube	0	0	0	1.0	1.74	1.55	2.73	5.925	3.9912	6.68e-2	0.243
Air cooler	-	CS	0	0	0	1.0	0.966 0	1.210	1.0	2.176	4.034	0.2341	4.970e-2
K-100	Rotary with gas engine drive	SS	0	0	0	1.0	-	-	-	5.0	5.0355	-1.8002	0.8253
K-101	Centrifugal with expander drive	CS	0	0	0	1.0	-	-	-	2.8	2.29	1.36	-0.1027
K-102 K-103	Centrifugal with gas engine drive	CS	0	0	0	1.0	-	-	-	3.4	2.29	1.36	-0.1027
V-100	Separator	CS	0	0	0	1.452	2.25	1.82	1	10.44	3.4974	0.4485	0.1074

Appendix C: Optimum values of the design variables

Table 15: Optimum optimization variables of feed A at low NGL to Gas price ratio

Demethanizer pressure (psia)	T_{10} (°F)	$\dot{M}_8$ (lbmol/hr)	$\dot{M}_{5out2}$ (lbmol/hr)	$P_{Economizer}$ (psia)	T_2 (°F)	P_{RG2out} (psia)	$\dot{M}_8$ (lbmol/hr)	T_{12out} (°F)
100	-140.0	2116	281.7	--	--	--	--	--
215	-92.5	4200	280.0	66.13	2.30	--	--	--
450	-75.0	5000	281.5	62.95	27.00	--	--	--

Table 16: Optimum optimization variables of feed D at low NGL to Gas price ratio

Demethanizer pressure (psia)	T_{10} (°F)	$\dot{M}_8$ (lbmol/hr)	$\dot{M}_{5out2}$ (lbmol/hr)	$P_{Economizer}$ (psia)	T_2 (°F)	P_{RG2out} (psia)	$\dot{M}_8$ (lbmol/hr)	T_{12out} (°F)
100	-71.5	2168	3500	62.84	35.95	--	--	--
215	-59.0	2873	3071	44.31	24.40	--	--	--
450	-43.0	3753	1366	98.00	56.35	--	--	--

Table 17: Optimum optimization variables of feed A at low NGL to Gas price ratio

Demethanizer pressure (psia)	T_{10} (°F)	$\dot{M}_8$ (lbmol/hr)	$\dot{M}_{5out2}$ (lbmol/hr)	$P_{Economizer}$ (psia)	T_2 (°F)	P_{RG2out} (psia)	$\dot{M}_8$ (lbmol/hr)	T_{12out} (°F)
100	-144.2	1797	280.0	--	--	128.2	819.7	-199.9
215	-102.0	3500	280.0	89.26	10.00	--	--	--
450	-71.0	6500	282.0	37.25	23.00	--	--	--

Table 18: Optimum optimization variables of feed D at low NGL to Gas price ratio

Demethanizer pressure (psia)	T_{10} (°F)	$\dot{M}_8$ (lbmol/ hr)	$\dot{M}_{5out2}$ (lbmol/hr)	$P_{Economizer}$ (psia)	T_2 (°F)	P_{RG2out} (psia)	$\dot{M}_8$ (lbmol/hr)	T_{12out} (°F)
100	-70.0	3800	4262	75.02	37.51	--	--	--
215	-63.0	2634	3486	72.58	25.82	--	--	--
450	-44.0	3015	1218	74.45	67.93	--	--	--

Vita

Balsam Swaidan was born in 1991, in Ajman, United Arab Emirates. She was educated in Ajman and graduated in 2009 with a score of 97% and enrolled in American University of Sharjah (AUS). She holds a bachelor's degree in Chemical Engineering and graduated in Spring 2013. She joined the MSc program of Chemical Engineering at the American University of Sharjah in Fall 2013. She has worked as a teaching assistant in the Chemical Engineering Department at AUS from 2013 to 2015. Currently, she is working as a graduate process integrity engineer in Asset Integrity Engineering, Sharjah.